



Designing cooperative interaction of automated vehicles with other road users in mixed traffic environments

interACT D.2.2. Final description of psychological models on human-human and human-automation interaction

Work package	WP2: Psychological Models on Human Interaction and Intention Recognition Algorithms
Task(s)	Task 2.2: Development of human-human and human automation interaction models (qualitative and quantitative)
Authors	Andre Dietrich (TUM), Klaus Bengler (TUM), Gustav Markkula (ITS Leeds), Oscar Giles (ITS Leeds), Yee Mun Lee (ITS Leeds), Jami Pekkanen (ITS Leeds), Ruth Madigan (ITS Leeds), Natasha Merat (ITS Leeds)
Dissemination level	Public (PU)
Status	Final, approved by EC
Due date	31/08/2019
Document date	02/09/2019
Version number	1.0



This work is part of the interACT project. interACT has received funding from the European Union’s Horizon 2020 research and innovation programme under grant agreement no 723395. Content reflects only the authors’ view. The Innovation and Networks Executive Agency (INEA) is not responsible for any use that may be made of the information it contains.

Table of contents

Glossary of terms	6
List of abbreviations and acronyms	7
Executive Summary	8
1. Introduction	9
1.1.1 Purpose and scope.....	9
1.1.2 Intended readership	10
1.1.3 Relationship with other interACT deliverables	10
2. Human-human interaction: Results from the observation studies	11
2.1 Defining interaction in traffic [D2.1]	11
2.2 Methods and previous results [D2.1]	13
2.2.1 Recapitulation of main findings in D2.1.....	15
2.3 Further results from data from the observation study	15
2.3.1 Cross-cultural findings from observation protocol and questionnaire	15
2.3.2 Shared space evaluation in Leeds	16
2.3.3 T-Junction observation in Germany.....	17
2.4 Discussion	19
3. Understanding road user behaviour	22
3.1 Human perception of vehicles in traffic	22
3.1.1 Implicit communication	23
3.1.2 Explicit communication	24
3.2 Results from controlled experiments in VR simulators.....	25
3.2.1 Effects of Deceleration Strategy and Jerk on Pedestrian Crossing Behaviour (Dietrich et al., 2019).....	25
3.2.2 Effects of Deceleration Distance and Presence of an eHMI on Pedestrian Crossing Behaviour and Perception (Dietrich et al., submitted 2019).....	27
3.2.3 Analysis of Gap Acceptances and Effects of Deceleration and Driver Attentiveness on Pedestrian Crossing Behaviour	29
3.3 Visual perception and its effect on interaction in traffic.....	30
4. Quantitative modelling of human-automation interaction	31
4.1 Objectives and research questions.....	31
4.2 Methods	32
4.2.1 Data collection	32

4.2.2	Models.....	37
4.3	Results and discussion.....	42
4.3.1	Model fits for the variable-drift diffusion models	42
4.3.2	Statistical analyses of the impact of distance and deceleration cues on behaviour.....	50
4.3.3	Model fits for the threshold distribution models	52
4.3.4	Relationships between scenario kinematics and subjective safety ratings	63
4.4	Conclusions.....	67
4.4.1	RQ1: Can the originally proposed VDDM framework capture the human behaviour in the studied crossing/turning scenarios?	67
4.4.2	RQ2: Can the models be scaled down to less complex versions?.....	67
4.4.3	RQ3: Can the same basic type of model be used both for pedestrian crossing and driver turning decision-making?.....	67
4.4.4	RQ4: Can the same basic type of model be used both for UK and Japanese road users, and if yes do the models need to be parameterised differently?	67
4.4.5	RQ5: To capture effects of available gap on crossing/turning behaviour, is it enough to consider only time to arrival, or should distance cues also be considered?.....	68
4.4.6	RQ6: To capture effects of vehicle deceleration on crossing/turning behaviour, is it enough to consider only time and/or distance gaps, or are direct cues describing deceleration also needed?	68
4.4.7	RQ7: Are there correlations between the kinematical conditions at crossing/turning and subjective ratings of perceived safety?.....	68
4.5	Simulation software	68
4.6	Future work	71
5.	Summary & outlook	72
6.	References	73
Annex 1:	Road crossing behaviour models – simulation software.....	76
	Overview	76
	Running model simulations from the GUI	77
	Running model simulations programmatically.....	81

Index of figures

Figure 1: Relationship with other interACT Work Packages	10
Figure 2: An illustration of how four types of interaction-relevant road user behaviours relate to each other (D2.1).....	12
Figure 3: Pictures from the locations used for use cases 1 and 2. Top left: Google Maps image from Leeds (UK), top right from Munich (Germany), bottom picture from Athens (Greece) [D2.1].....	13
Figure 4: (Left) Aerial satellite image of observation site. (Right) Location of observation site within Leeds (UK) urban centre	16
Figure 5: Depiction of the observed T-Junction. (Dietrich & Ruenz, 2018)	18
Figure 6: Typical sequence of a driver on the main road increasing headway to let another vehicle from the side road merge (numbers represent velocity in km/h).....	19
Figure 7: Implicit communication capabilities of a vehicle.....	23
Figure 8: Simplified depiction of visual communication capabilities from vehicles towards other road users.....	25
Figure 9: Interaction diagrams of main factors pitch and strategy. (Dietrich et al. 2019)	26
Figure 10: Interaction diagrams of main factors pitch and strategy. (Dietrich et al., submitted 2019). 28	
Figure 11: The VR scene in the pedestrian crossing scenario.....	34
Figure 12: The VR scene in the driver turning scenario. The two insets show a birds-eye-view (not seen by the participants), as well as the view across the intersection at the start of each scenario.....	36
Figure 13: Illustration of the three model types tested here.	38
Figure 14: Illustration of the threshold distribution model (TDM) in a scenario with an approaching vehicle.....	40
Figure 15: Human pedestrian crossing times (gray bars) and probability distribution predictions by fitted VDDM variants (solid lines), across time elapsed in the scenario (x axis, seconds), in two example <i>Constant velocity</i> scenarios with same <i>TTAinit</i> but different <i>vinit</i> and <i>Dinit</i>	44
Figure 16: Human pedestrian crossing times (gray bars) and probability distribution predictions by fitted VDDM variants (lines), across time elapsed in the scenario (x axis, seconds), in two example <i>Decelerate to a stop</i> scenarios with same <i>TTAinit</i> and <i>vinit</i> but different <i>Dstop</i>	45
Figure 17: Human pedestrian crossing times (gray bars) and probability distribution predictions by fitted VDDM variants (lines), across time elapsed in the scenario (x axis, seconds), in the <i>Decelerate without stopping</i> scenario with <i>TTAinit</i> = 3 s.....	46
Figure 18: Human driver turning times (gray bars) and probability distribution predictions by fitted VDDM variants (solid lines), across time elapsed in the scenario (x axis, seconds), in two example <i>Constant velocity</i> scenarios with same <i>TTAinit</i> but different <i>vinit</i> and <i>Dinit</i>	48
Figure 19: Human driver turning times (gray bars) and probability distribution predictions by fitted VDDM variants (solid lines), across time elapsed in the scenario (x axis, seconds), in two example <i>Decelerate to a stop</i> scenarios with same <i>TTAinit</i> but different <i>vinit</i> , <i>Dinit</i> , and <i>Dstop</i>	49

Figure 20: Human driver turning times (gray bars) and probability distribution predictions by fitted VDDM variants (lines), across time elapsed in the scenario (x axis, seconds), in the *Decelerate without stopping* scenario with ***TTAinit*** = 5 s. 50

Figure 21: The ***tpass*** (generalised TTA or TTC) and ***TR*** (reaction time) probability distributions obtained when fitting the TDMs to the UK (left two columns) and Japanese (right two columns) pedestrian crossing scenario. 55

Figure 22: Human pedestrian crossing times (grey bars) and probability distribution predictions by fitted TDM variants (solid lines), across time elapsed in the scenario (x axis, seconds), in two example *Constant velocity* scenarios with same ***TTAinit*** but different ***vinit*** and ***Dinit***. 56

Figure 23: Human pedestrian crossing times (gray bars) and probability distribution predictions by fitted TDM variants (lines), across time elapsed in the scenario (x axis, seconds), in two example *Decelerate to a stop* scenarios with same ***TTAinit*** and ***vinit*** but different ***Dstop***. 57

Figure 24: Human pedestrian crossing times (grey bars) and probability distribution predictions by fitted TDM variants (lines), across time elapsed in the scenario (x axis, seconds), in the *Decelerate without stopping* scenario with ***TTAinit*** = 3 s. 58

Figure 25: The ***tpass*** and ***TR*** probability distributions obtained when fitting the TDMs to the UK (left two columns) and Japanese (right two columns) driver turning scenario. 60

Figure 26: Human driver turning times (gray bars) and probability distribution predictions by fitted TDM variants (solid lines), across time elapsed in the scenario (x axis, seconds), in two example *Constant velocity* scenarios with same ***TTAinit*** but different ***vinit*** and ***Dinit***. 61

Figure 27: Human driver turning times (gray bars) and probability distribution predictions by fitted TDM variants (solid lines), across time elapsed in the scenario (x axis, seconds), in two example *Decelerate to a stop* scenarios with same ***TTAinit*** but different ***vinit***, ***Dinit***, and ***Dstop***. 62

Figure 28: Human driver turning times (gray bars) and probability distribution predictions by fitted TDM variants (lines), across time elapsed in the scenario (x axis, seconds), in the *Decelerate without stopping* scenario with ***TTAinit*** = 5 s. 63

Figure 29: Subjective ratings of agreement with the statement “It was safe to cross before the vehicle” (blue dots) provided after trials from three different example pedestrian crossing scenarios, as a function of time at which the participants initiated crossing in the given trial. 65

Figure 30: Subjective ratings of agreement with the statement “It was safe to cross before the vehicle” (blue dots) provided after trials from three different example driver turning scenarios, as a function of time at which the participants initiated turning in the given trial. 66

Figure 31: The graphical user interface of the road crossing behaviour simulation software provided with this deliverable. 69

Figure 32: The two types of scenarios modelled in the simulation software. 77

Figure 33: GUI for setting model parameters and running simulations. 78

Figure 34: GUI for exploring model simulation results. 80

Index of tables

Table 1: Overview of conducted experiments [D2.1]	14
Table 2: Deceleration strategies evaluated in the VR study (see Dietrich et al. 2019)	26
Table 3: Braking distances and corresponding maximum decelerations evaluated in the VR study (see Dietrich et al. 2019)	27
Table 2: Overall experiment design and participant demographics for the data collection carried out to support model development.	33
Table 3: Pedestrian crossing scenario variants.	35
Table 4: Driver turning scenario variants.	37
Table 5: VDDM fits for the UK pedestrian crossing scenario. See the text for meanings of symbols and formatting.	42
Table 6: VDDM fits for the Japanese pedestrian crossing scenario. See the text for meanings of symbols and formatting.	42
Table 7: VDDM fits for the UK driver turning scenario. See the text for meanings of symbols and formatting.	46
Table 8: VDDM fits for the Japanese driver turning scenario. See the text for meanings of symbols and formatting.	46
Table 9: Effect of the approaching vehicle’s initial distance on pedestrian crossing timing.	51
Table 10: Effect of the approaching vehicle’s initial distance on driver turning timing.	51
Table 11: Effect of the approaching vehicle’s final stopping distance on pedestrian crossing timing. ...	52
Table 12: TDM fits for the UK pedestrian crossing scenario. See the text for meanings of symbols and formatting.	52
Table 13: TDM fits for the Japanese pedestrian crossing scenario. See the text for meanings of symbols and formatting.	53
Table 14: TDM fits for the UK driver turning scenario. See the text for meanings of symbols and formatting.	58
Table 15: TDM fits for the Japanese driver turning scenario. See the text for meanings of symbols and formatting.	58
Table 16: A listing of the types of analysis plots accessible via the simulation software GUI, together with explanations and possible interpretations and uses. A and C refer to the approaching and crossing/turning road users, respectively.	70

Glossary of terms

Term	Description
Vulnerable Road User (VRU)	Road users with a higher fatality rate per accident than other groups. In particular, pedestrians, bicycles, motorised two-wheelers and non-motorised traffic.
Mixed Traffic	Usually referred to traffic consisting of different types of road users (such as pedestrians, busses, cars, etc.). Also used in the context of traffic consisting of automated vehicles mixed and human road users.
Transition Phase	Projected or theoretical time frame between the first vehicles with higher automated driving functions (SAE3+) being integrated into traffic and the majority of motorized traffic is being automated.
Reaction	Reaction [of one road user to other road users]: Road user A is said to have reacted to road user B if A's behaviour can be interpreted as A having perceived B and A's behaviour having been affected to some extent by B.
Interaction	Interaction [between road users]: Road users A and B are said to be interacting if they are both reacting to one another (by the above definition of reaction).
Traffic Conflict	An observable situation in which two or more road users approach each other in space and time to such an extent that a collision is imminent if their movements remain unchanged.
Edging	Moving forward with very low velocity usually to indicate a desired trajectory (e.g. turning). Edging is mostly used by drivers, trying to pull out of a parking space with limited vision or while turning on congested priority lanes.
eHMI	External Human Machine Interface. Any interface perceivable from the exterior of a vehicle to communicate and/or interact with another human road user. This includes conventional methods, such as honks or the turn indicator, but also novel concepts projecting images on the ground.

List of abbreviations and acronyms

Abbreviation	Meaning
AV	Automated Vehicle
RU	Road User
HRU	Human Road User
VRU	Vulnerable Road User
D	Deliverable
WP	Work package
eHMI	External Human Machine Interface
MA	Movement Achieving
MS	Movement Signalling
PA	Perception Achieving
PS	Perception Signalling
LiDAR	Light detection and ranging
VR	Virtual Reality
ANOVA	Analysis of variance
LED	Light-emitting diode
HMD	Head-Mounted Display
VDDM	Variable-drift diffusion model
RQ	Research Question
TTA	Time to arrival
DDM	Drift diffusion model
C-VDDM	Connected variable-drift diffusion model
D-VDDM	Dual variable-drift diffusion model
S-VDDM	Single variable-drift diffusion model
TTC	Time to collision
CT	Crossing time
PSO	Particle swarm optimization
TDM	Threshold distribution model
GUI	Graphical user interface

Executive Summary

Automated Vehicles (AVs) have seen rapid technological development over the last decade and will soon be deployed on public roads. However, road traffic is unlikely to become fully automated in the near future. Instead, AVs will share the road space with human road users (HRUs), including cyclists, pedestrians and drivers. A major challenge in the development of AVs is understanding how these vehicles should interact with HRUs to ensure safe and efficient traffic flow. interACT aims to understand how interactions unfold between road users, in order to ensure the safe integration of AVs into mixed traffic environments.

This document describes the final psychological models on human-human and human-automation interaction developed in Work Package 2 (WP2) of the interACT project. At first, the observational studies conducted in Task 2.1 and reported in D2.1 are summarized and additional results of further analyses are presented. Overall results from the observation studies show that explicit communication is utilized rarely in urban traffic encounters, as road users try to avoid conflicts by adapting their kinematic behaviour. Pedestrians tend to base their decision making using motion cues from the vehicles, rather than establishing eye contact and waiting for gestures from the driver. A velocity threshold for interaction was identified at 25-35 km/h – above, interaction is unlikely to occur and sees road users trying to find appropriate gaps to either cross or merge with the traffic.

Secondly, this deliverable reports the project research on perception of vehicles in traffic conducted in simulator studies, to understand, which cues could potentially enhance the interaction. A defensive driving style and early onset of deceleration leads to a faster recognition of a yielding intent by the other traffic participant. Furthermore, external Human-Machine Interfaces expedite the perception of a yielding intent and are therefore likely to increase traffic flow.

Thirdly, the deliverable presents an approach to quantitatively model interaction. The underlying research questions, and methods to generate appropriate data for the modelling are presented and discussed. The created simulation software modelling interaction is publicly available for download and described in the annex.

The work of WP 2 reported in this deliverable influences the final tuning of the interaction controller of the Cooperation and Communication Planning Unit (CCPU) and sets the basis for the WP6 related evaluation work.

1. Introduction

1.1.1 Purpose and scope

A safe integration into current urban traffic conditions can be achieved by an expectation conforming AV behaviour and communication capabilities replacing a driver in control. Therefore, an understanding of what is expected by human traffic participants is the bases for the AV design.

The naturalistic observation study described in Deliverable 2.1 (Dietrich et al., 2018) revealed how different RUs interact with each other in specific use-cases within current urban traffic. Sequence diagrams have been created to understand when and how RUs communicate implicitly and explicitly. To further increase the understanding of human-human interaction and identify how automation might influence this interaction, qualitative and quantitative models of interaction are required.

Deliverable 2.2 “Final description of psychological models on human-human and human-automation interaction” presents the final outcome of WP 2 related work and provides a description of human road user behaviour in interaction demanding traffic situations. Chapter 2 summarizes the observation studies, giving a brief overview of the utilized methods and their advantages and disadvantages. Factors influencing road user behaviour in interaction demanding situations are described in Chapter 3. Chapter 4 describes the process of quantitatively modelling human-human and human-automation interaction giving details into the parametrization and model fitting. The achieved results are summarized in Chapter 7.

1.1.2 Intended readership

This deliverable gives an insight into the modelling work of WP 2 and reports the results of the final models on human-human and human-automation interaction, partly based on the results reported in Deliverable 2.1. Therefore, this document serves primarily as an input for all interACT partners from WP 3, 4, 5, and 6, presenting relevant information on the concrete human models that influences the final demonstrator set-up and the evaluation work. It also serves as a documentation of the research work in WP 2 for our Project Officer, the reviewers and the European Commission.

As this deliverable is public, the document is also written for our stakeholders, for other researchers and industrial partners who are interested to know more about the project’s modelling approach and the final results of the research work.

1.1.3 Relationship with other interACT deliverables

This deliverable is built on the results and definitions from Task 2.1 “Naturalistic, cross-cultural observation of present human-human interactions”, which were described within Deliverable 2.1. The models address the use-cases and scenarios defined within D1.1 “Definition of interACT use cases and scenarios”. To evaluate human-automation interaction, the interaction strategies described in D4.1 and D4.2 “Preliminary / Final interaction strategies for the interACT Automated Vehicles” were utilized. The developed models are based on the observations described in D2.1 and on simulator experiments. Their applicability and generalizability will be evaluated with the demonstrator-vehicle studies conducted in WP6 “Evaluation & Impact Assessment of Human-Vehicle Interaction”.

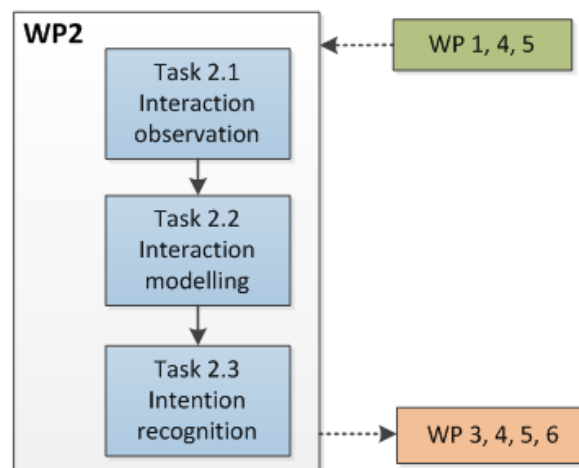


Figure 1: Relationship with other interACT Work Packages

2. Human-human interaction: Results from the observation studies

This chapter gives a summary about how interaction is defined within interACT and insights into the observation study conducted in D2.1. Further analyses of the data gathered during the observation study is presented and followed by a discussion on the utilized methods.

2.1 Defining interaction in traffic [D2.1]

This section summarizes the definition of interaction and interaction-relevant road user behaviour relevant for this deliverable. A more detailed and in-depth description of the defined terminology can be found in D2.1.

Interaction between road users is defined as follows:

“Road users A and B are said to be interacting if they are both reacting to one another [...]”

Reaction can be described as road user “A having perceived B and A’s behaviour having been affected to some extent by B”.

Based on these definitions, four main types of interaction-relevant road user behaviour were defined in D2.1 as:

Movement-achieving (MA) behaviour: Behaviour that moves a road user in the world.

Movement-signalling (MS) behaviour: Behaviour that can be interpreted as giving information on how a road user intends to move in the future.

Perception-achieving (PA) behaviour: Behaviour that determines what a road user perceives.

Perception-signalling (PS) behaviour: Behaviour that can be interpreted as giving information on what a road user is perceiving.

In traffic encounters these behaviours are utilized by road users to achieve their individual goals while avoiding potential conflicts by communicating and interacting with other traffic participants. Figure 2 shows how the main types of interaction-relevant road user behaviour overlap, while providing examples from behaviour typically found in traffic.

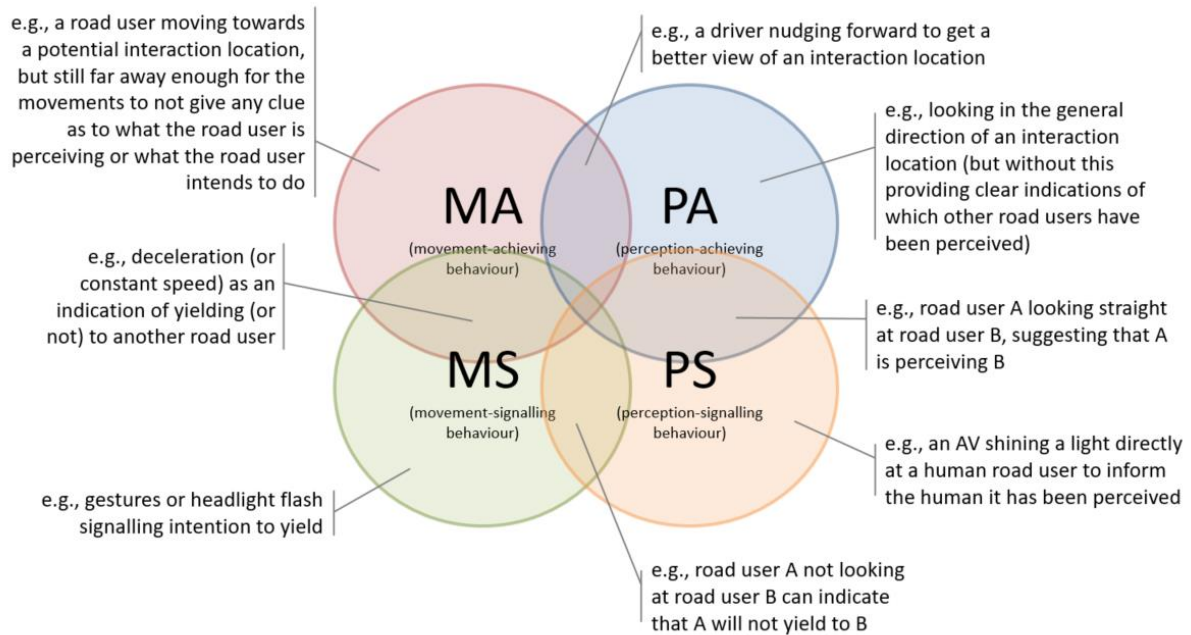


Figure 2: An illustration of how four types of interaction-relevant road user behaviours relate to each other (D2.1).

Two other concepts widely used within interACT and found in other research are implicit and explicit communication. While explicit communication refers to clearly visible and intentional means to transmit a message to other RUs (e.g. flashing the headlights, gestures), implicit communications is understood as intentionally and unintentionally communicating through one’s appearance, position and movement (e.g. decelerating to indicate a yielding intention. Also the size of an approaching vehicle can influence the action of other road users (de Clercq et al., 2019)).

These two concepts were defined using the four main types of RU behaviour:

Implicit communication: A behaviour which is at the same time **both achieving and signalling** movement and/or perception.

Explicit communication: A behaviour signalling perception and/or movement without at the same time achieving either of these.

2.2 Methods and previous results [D2.1]

To study road user in current traffic conditions, an observational study was conducted in Munich, Leeds and Athens at locations resembling the use cases defined in D1.1. Figure 3 depicts three locations for the observations of use-cases 1 and 2 – pedestrian-vehicle and vehicle-vehicle interaction at intersections.



Figure 3: Pictures from the locations used for use cases 1 and 2. Top left: Google Maps image from Leeds (UK), top right from Munich (Germany), bottom picture from Athens (Greece) [D2.1]

Five different methods were used to observe current traffic interactions (an in-depth description can be found in D2.1):

Manual observations of interactions. Three researches on the ground noted the sequence of an interaction-requiring traffic encounter into an HTML app. This method allows to capture the

occurrence of explicit and implicit communication and to put the observed events into a sequence of occurrence.

Questionnaires for pedestrians. After pedestrian-vehicle encounters, one of the researchers on the ground followed the pedestrian involved in the interaction to understand how individual pedestrians perceived the preceding encounter and to assess their general traffic behaviour using the Adolescent Road User Behaviour Questionnaire.

High angle videos. Cameras were mounted on higher ground to record videos of the interactions at the specified locations. These videos allow to review interactions of the manual observations and can further be used to extract positional data using Computer Vision algorithms.

Ground based LiDAR. To acquire positions and velocities of interacting road users, a ground based LiDAR was deployed. This was especially helpful in situations where no nearby building was high enough or accessible for video recordings.

Running commentary. Controlled experiments with drivers who were asked to drive a specific route. After the experiment (including eye-tracking and video recordings) drivers were asked to comment while reviewing the video of their driving. While this method technically is not a naturalistic observation, it provided insights into drivers’ subjective perception of interaction-demanding traffic encounters.

Overall seven sub-studies were conducted to observe current interactions in traffic (see Table 1).

Table 1: Overview of conducted experiments [D2.1]

Research institute	Sub-Study	Utilized methods
ICCS, Athens, Greece	Observation: urban intersection (use case 1 & 2)	Video, observation protocol, questionnaires
ICCS, Athens, Greece	Controlled experiment with drivers (all use cases)	Video from within vehicle, eye tracking, subjective reports by drivers
ITS Leeds, UK	Observation: urban intersection (use case 1 & 2)	Video, observation protocol, questionnaires, LiDAR
ITS Leeds, UK	Observation: shared space (use case 3 & 4)	Video, observation protocol
TUM, Munich, Germany	Observation: urban intersection (use case 1 & 2 ¹)	Video, observation protocol, questionnaires, LiDAR
TUM, Munich, Germany	Observation: shared space (use case 3 & 4)	Video, observation protocol
TUM, Munich, Germany	Observation: sub-urban intersection (use case 2)	LiDAR, observation protocol

¹ The intersection in Germany had very little vehicle-vehicle interactions. Therefore, the observation for use case 2 was repeated at another location.

2.2.1 Recapitulation of main findings in D2.1

Explicit communication is utilized rarely in traffic conditions requiring interaction. This is due to road users adapting their movement achieving behaviour ahead of time. Thus, current urban is mostly based on conflict avoidance rather than reciprocal interaction. Explicit communication was utilized whenever the kinematic adaptation did not result in the anticipated behaviour and/or the relative velocity and distance was low. Drivers mostly used waiving hand gestures to interact with pedestrians and other drivers in close proximity and flashed their headlights for other drivers to communicate their yielding intent early. Edging, i.e. moving forward with a very low velocity, was found to be a very effective method to resolve standstills or to force one's way onto a prioritized road.

The analysis of questionnaires provided insights into how approaching vehicles are perceived by pedestrians. Pedestrians mostly base their crossing decisions on speed and distance of the approaching vehicle. To indicate the intention to cross the street, pedestrians mostly turned their head towards the oncoming traffic and make a step forward. The manual observations allowed to recreate sequences of individual interactions. Summarized over all comparable interactions, sequence diagrams were created for vehicle-pedestrian and vehicle-vehicle encounters. Observed road user behaviour was formulated into recommendations for automated vehicles in the observed use-cases within D2.1 (Dietrich et al. 2018).

2.3 Further results from data from the observation study

This section details, which work on the further work on the dataset of the observation studies was conducted after D2.1.

2.3.1 Cross-cultural findings from observation protocol and questionnaire

The observation protocol and questionnaire (D2.1) were further analysed to investigate whether, and to what extent, explicit communication was used between pedestrians and drivers while crossing the road at six observed locations in Leeds, Athens and Munich. Among 989 observations, it was shown that the explicit communication techniques, such as honking, flashing, headlights, or hand gestures rarely occurred. Questionnaire results also revealed that pedestrians were more likely to use vehicle-based movement information than driver-based information to judge how safe it was to cross. (Lee et al., under review).

These findings were consistent across the observed locations, which had a speed limit of 50km/h, suggesting that in these situations road users rely more on implicit communication in their decision making. This may mean that eHMI is not necessary in these faster moving situations. However, explicit communication was still reported and observed on occasion, therefore further study is needed to consider the specific circumstances in which this arises. In addition, as shown in section 2.3.2, more

explicit communication might still occur in a shared space with a lower speed limit or in deadlock situations.

2.3.2 Shared space evaluation in Leeds

In Deliverable 2.1, the selection of observation locations for the interACT project was outlined. Use cases 3 and 4 (see Wilbrink et al., 2018) focus on understanding pedestrian-vehicle and vehicle-vehicle interactions in shared spaces. In order to develop models of common communication behaviours in these types of situations, observation protocols administered at the shared space location in the UK were analysed. 66 pedestrian-driver interactions and 124 driver-driver interactions were observed at a busy train station car-park location in Leeds (see Figure 1), with three trained observers capturing information on the number of pedestrians, their demographic information, the position and actions of any vehicles, and the human and vehicle communication signals used (both implicit and explicit) . More detail on the procedures used can be found in D2.1.

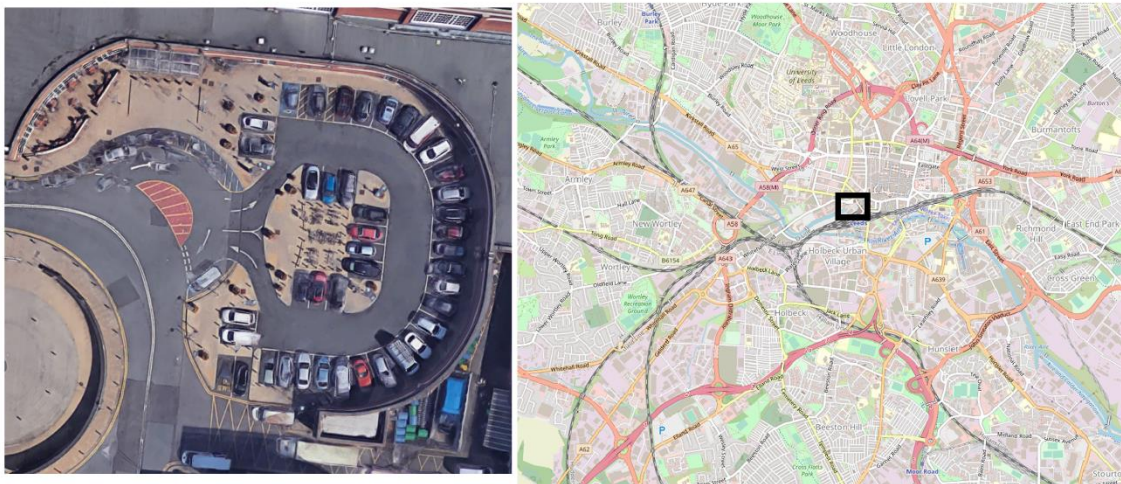


Figure 4: (Left) Aerial satellite image of observation site. (Right) Location of observation site within Leeds (UK) urban centre

Pedestrian-Vehicle Interactions

Results indicated that explicit human communication gestures such as hand or head movements were relatively rare in pedestrian-driver interactions by either road user, occurring in only 12-17% of analysed interactions. However, the driver's behaviour appeared to be influenced by whether the pedestrian looked at them or their vehicle. Drivers were more likely to either stop completely or continue at their current speed if the pedestrian looked towards them, whereas they were more likely to slow down without stopping if the pedestrian did not look towards them. This suggests that when a pedestrian was not looking in their direction, the driver experienced uncertainty as to whether they had been seen and reduced their speed accordingly (Uttley et al., in preparation).

An investigation of which road user took priority in interactions i.e. which user slowed or stopped to allow the other to pass in front, found that pedestrians took priority in 78% relevant interactions, a much higher proportion than has been found in other studies (e.g. Varhelyi, 1998; Crowley, Koch, and van Houten, 2011). This suggests that the low speed shared-space location leads to a change in pedestrian-vehicle interactions, with drivers' providing pedestrians with more priority when compared to on the open road or at intersections. Our observations did not suggest that this additional priority was a result of pedestrians looking at the driver, with no differences in priority emerging between pedestrians who looked at the driver compared to those who did not. This is in contrast to previous research on pedestrian crossing scenarios (Gueguen, Meineri & Eyssartier, 2015) which had found that looking toward the driver and making eye contact increased the likelihood that the driver would yield. The increased ambiguity of the shared space scenario, and the slow travelling speeds may have contributed to this finding. Priority was also influenced by the number of pedestrians involved, with drivers more likely to give priority to a group of pedestrians than a single pedestrian, a finding that supports previous research showing an increase in driver yielding behaviour when groups of pedestrians are waiting to cross a road, compared with a single pedestrian [e.g. Himanen and Kulmala, 1988; Sucha, Dostal, & Risser, 2017).

Driver-Driver interactions

Explicit vehicle-based signals were used in a third of interactions between drivers, but hand gestures were only used in approximately 10% of interactions, suggesting that the development of communication mechanisms for automated vehicles may not have to replace explicit communication from the driver themselves (Uttley et al., in preparation). However, the results also showed that drivers would frequently turn and look towards the other vehicle involved in an interaction, and this looking behaviour influenced how the other driver acted. Drivers were more likely to slow down without stopping completely if another driver was not looking towards them. Similar to the pedestrian-interactions, the ambiguity about priority in the shared space may have led drivers to be more cautious when they were unsure if they had been seen or not. Use of vehicle-based signals by one driver was associated with the other driver slowing or stopping, or giving priority to the signalling driver. This confirms that signals from a vehicle can help resolve interactions, providing justification for ongoing efforts to develop external signal-based communication methods for automated vehicles (Uttley et al., in preparation).

2.3.3 T-Junction observation in Germany

Vehicle-vehicle interaction on intersections occurs mostly if one driver on a not-prioritized road is trying to merge onto a road with higher priority. In normal traffic conditions, the driver would wait until a large enough gap opens up and merge into the traffic on the main road. If the traffic density increases, less appropriate inter-vehicle are available to merge. To understand how drivers merge onto priority roads in high density traffic, a T-Junction in a German suburban area, which is very busy in peak times, was observed. As the surrounding buildings were not high enough to enable cameras

recordings without capturing licence plates, the ground LiDAR described in D2.1 (also in Dietrich & Ruenz, 2018) was primarily used to obtain positional information of all surrounding vehicles.

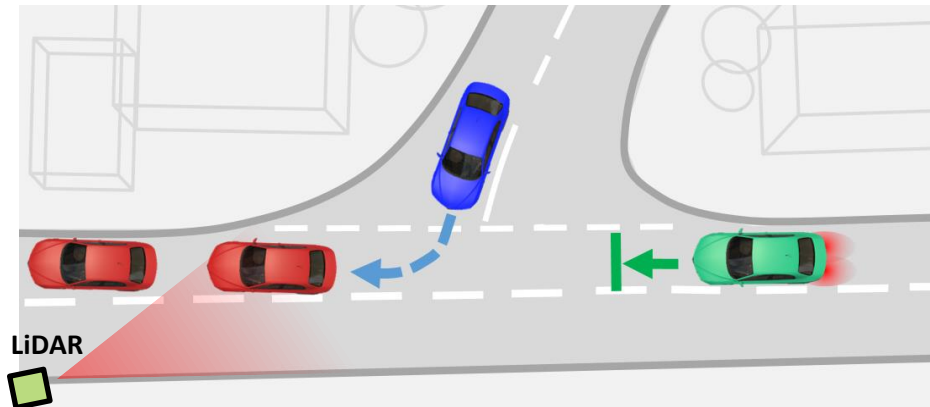


Figure 5: Depiction of the observed T-Junction. (Dietrich & Ruenz, 2018)

The T-Junction depicted in Figure 5 consisted of a straight main road, where traffic was allowed to drive up to 50 km/h. The merging side road had a speed limit of 30 km/h. Early morning traffic was mostly headed towards Munich and congestions build up regularly on the main road. Over three days, 4 hours of LiDAR data was collected, with 60 explicit interactions being also manually observed using the interACT HTML app (see D2.1).

The high traffic density of the rush hour lead to tailbacks, caused by a traffic light approximately 1.5 km after the intersection. Due to the large distance to the traffic light fully stopping traffic in close proximity, traffic around the intersection was fluent but slowed down:

- with little traffic ahead, vehicles along the main road were observed to pass the intersection at 50 – 60 km/h, occasionally peaking at 65 km/h
- Once the backlog built up, traffic on the main road slowed down to 15 – 30 km/h and only slowed down further, when vehicles on the main road tried to turn onto a fuel station right after the intersection.

While in normal traffic conditions, vehicles on the side road always relied on large enough gaps to merge onto the main road. Once congested conditions prevailed, cooperative behaviour was observed: some vehicles on the main road increased their headway to the leading vehicle, allowing turning traffic to merge and in some cases showing the yielding intent with a headlight flash. This process usually started at distances between 25 and 100 m towards the intersection. Once one vehicle started to let turning vehicles onto the road, usually the following vehicles started creating gaps as well leading to some sort of zip merging until either no vehicles were left on the side road or the road cleared up due to other traffic lights before the intersection. Figure 6 shows a view generated by the LiDAR with velocities in km/h written above the trajectory. The image on top left shows that the initial

velocities of the two highlighted vehicles on the main road is comparable. However, the driver in the second vehicle sees the waiting traffic on the side road and decides to increase his headway by not accelerating (top right). The headway increases to approximately 25m (bottom left) and the gap is accepted by the waiting driver (bottom right).

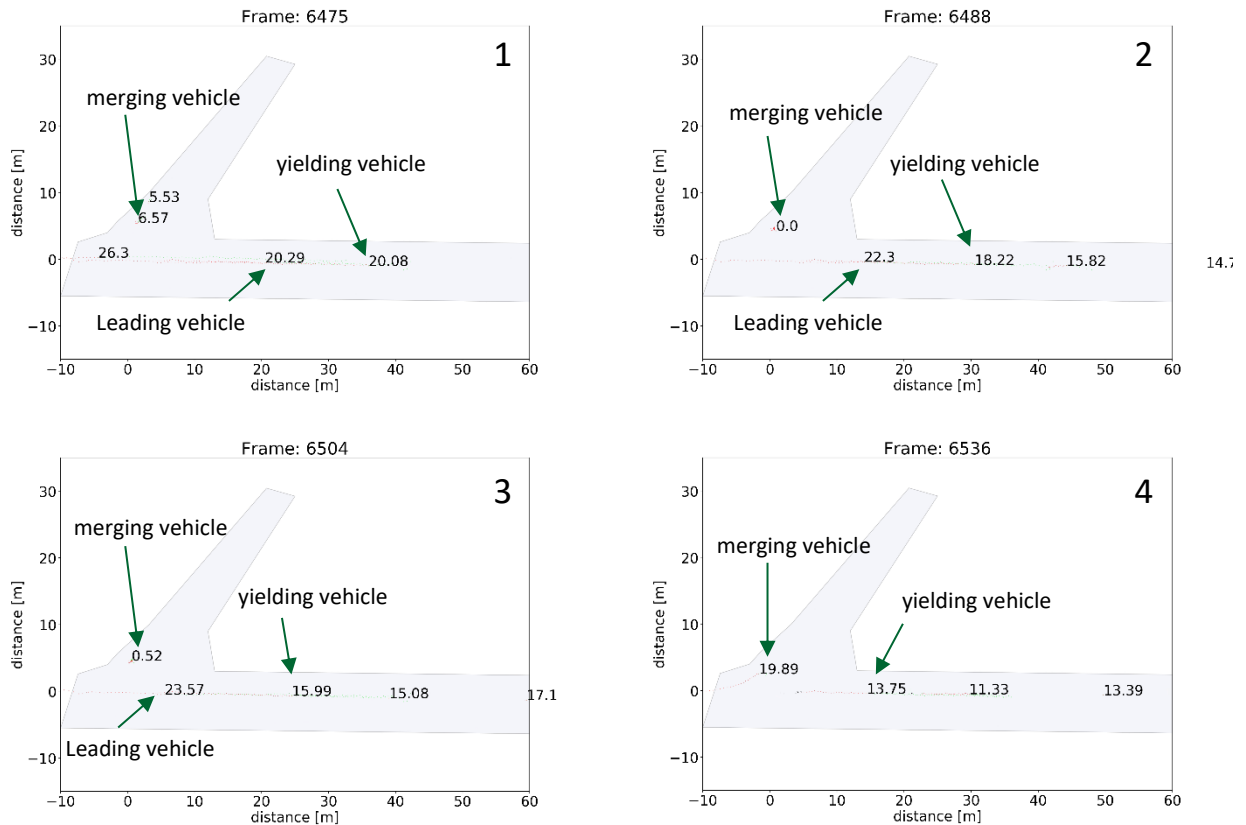


Figure 6: Typical sequence of a driver on the main road increasing headway to let another vehicle from the side road merge (numbers represent velocity in km/h).

This observation revealed that interaction only seems to occur in traffic, where velocity is greatly reduced due to high traffic density. A velocity threshold for interaction is likely to be between 25 and 35 km/h (see section 2.4 for limitations on measurement accuracy). Below this threshold road users were likely to let others merge in congested situations. Above the threshold, drivers on the main road did rarely decelerate to create sufficient gaps.

2.4 Discussion

With the observation studies a large set of data was generated, consisting of protocols and questionnaires as well as video and LiDAR recordings. While many key insights were found within the

observation studies, most of the data is still available for processing by future researches. The observation studies gave an insight into current traffic interactions and allow to conclude the following statements:

- External communication (and deliberate interaction) is utilized rarely on main road intersections. In these scenarios, conflict avoidance prevails.
- Road users rely mostly on implicit cues – this is consistent over the three countries, in which the observation took place (Greece, UK and Germany).
- Congested traffic leads to more cooperative behaviour. Once the velocity on main road falls below a certain threshold of 25 – 35 km/h, cooperative behaviour in the form of letting other traffic participants merge, can be observed.

The approach to observe traffic utilizing different method synchronized in time, proved to be an effective way to generate a holistic view on traffic in specific situations. However, every method has its advantages and disadvantages, which are described below, so future researchers can adapt to the challenges occurring when observing traffic. A more in-depth overview of the utilized Methodologies within interACT and the twinning project AVINTENT can be found in Portouli et al. 2019.

Questionnaires and interviews are a valuable tool, to get insights into the subjective decision making processes of pedestrians. In urban traffic, pedestrians are usually headed somewhere. Especially in the traffic condition, which sees the most occurrence of interaction – rush hour – pedestrians are unwilling to participate in the study. Up to 90% of the time, an observer approached a pedestrian that interacted with traffic, no answers were given, mostly due to a tight schedule of the pedestrians.

The **observation protocol app** enables to recreate sequences of recently observed interactions. However, as there are a lot of possible interaction paradigms and therefore buttons to press, using the app needs to be trained extensively to ensure an acceptable inter-rater reliability. The app allows to observe traffic with only personal effort and was used in further observations in Munich within the national @City project.

The **video recordings** were mostly used to recapitulate interactions observed using the app. An effort was made to extract positional and kinematic information from the observed road users. Tracking algorithms are complicated and suffer greatly from low resolution and high distortion. A higher resolution would increase the tracking accuracy greatly, but could raise data privacy concerns, as faces would become identifiable.



A **ground based LiDAR** is a valuable tool to gather kinematic information of traffic encounters without generating personalized data. However, the data suffers from view obstructions – all data, when traffic on the opposite lane was present, had to be disregarded, as the observed vehicles were invisible for the time it took the traffic to pass. The kinematic values of observed vehicles were very volatile, which could be enhanced in future research by utilizing a LiDAR with a higher resolution (more layers).

In general, the observation studies are a good way to get insights into current road user behaviour in interactive scenarios. However, the insights are hard to generalize towards other use cases or even other locations. Furthermore, understanding the underlying processes of interaction and thus communication would require a sheer amount of observational data and data processing. Therefore, controlled experiments are necessary, to understand the effects of explicit and implicit communication on road user behaviour.

3. Understanding road user behaviour

The observation study conducted within Task 2.1 gives a macroscopic view of the pre-defined use cases in current traffic. This allows to identify interactive situations, classify those and extract action sequences of interacting road users. However, generating an understanding how a single vehicle's position and velocity along with its means of communication affects the decision making of an interacting road user, would require a vast amount of observational data, as each observable encounter is somewhat unique. Therefore, controlled experiments are required to explore the individual effects of road user behaviour on interaction demanding situations. This chapter describes how different virtual reality experiments were set up to explore the effects of vehicle communication on pedestrian behaviour.

3.1 Human perception of vehicles in traffic

Interaction in traffic was defined in chapter 2.1 as the reciprocal reaction of road users to each other's behaviour, which itself was categorized in four categories. Once a road user's behaviour is perceivable by another one, it becomes a form of communication – regardless of whether an intention or awareness to communicate was present. Communication in traffic is comparable to human communication, especially the first axiom of Paul Watzlawick (2016) “one cannot not communicate” seems applicable as shown in the examples below.

Examples

Intentional/aware communication, no addressee:

A driver reversing out of a perpendicular parking with no vision of the road due to obstructions usually tries to slowly edge out onto the street. While at the beginning of the manoeuvre, other traffic participants are likely to bypass, the further the vehicle reverses onto the road, the more likely a vehicle will yield. Therefore, the reversing driver is knowingly communicating his intentions without even knowing, whether an addressee is present.

Unintentional/unaware communication:

Especially in jay walking scenarios with higher velocities (~50 km/h), pedestrians will cross the street, whenever they find a passable inter-vehicle gap. The distant vehicle itself communicates implicitly through its position and velocity that the gap is large enough to cross.

To examine the effects of communication in traffic it is key to explore, how vehicles are perceived by other road users. While multiple senses can perceive certain traffic situations (e.g. olfactory through

exhaust fumes, kinaesthetic when the own vehicle shakes due to aerodynamic effects after surpassing a larger vehicle), it is clear that traffic is mostly perceived visually and acoustically, with the visual sense being the main channel (Riemersma 1979). As the demonstrator vehicles will not use audible cues for different vehicle intentions, this chapter focuses on the visual perception of vehicles by other road users. Furthermore, only one use case – pedestrian vehicle interaction at a straight road section – is examined, to create a comparable and holistic understanding of pedestrian behaviour while minimizing confounding variables.

As described in D2.1 and chapter 2.1, communication can be divided into implicit or explicit communication and those forms are used in the interACT project for the communication with other road users (see interaction strategies and design described in D4.1 and D4.2). The two strategies are described in the following subsections and evaluated in section 3.2.

3.1.1 Implicit communication

There are limited ways, a driver can transmit an intention while within a vehicle. Implicit communication of a vehicle itself can be simplified by linking the geometric properties (see Figure 7) with perceivable motion.

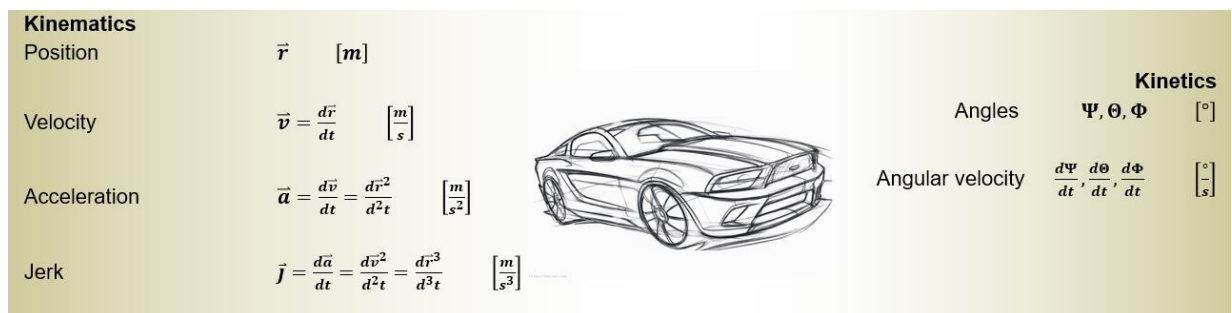


Figure 7: Implicit communication capabilities of a vehicle

While a driver controls the vehicle using the gas or brake pedal and the steering wheel, another road user visually perceives the approaching vehicle as a moving geometric object. While visual perception of humans is a complicated process in general, Figure 7 shows, which geometric parameters of a moving vehicle are distinguishable perceivable by an outside observer.

- The relative **position** of the vehicle in regards to the observer is determined by the size of the object and other environmental depth cues.
- The **velocity** of a vehicle is perceived by visual looming, i.e. the increasing size of an approaching object.
- The **acceleration**, i.e. the change of velocity, is harder to visually perceive through looming, but directly linked to the **rotation angle** of the vehicle. A decelerating vehicle is pitched slightly forward due to vehicle dynamics.

- **Jerk**, or the change of acceleration, is likely not directly perceivable due to visual looming by a pedestrian. However, the jerk translates into the rate of rotational change, or **angular velocity**.

For a pedestrian in a road crossing situation, vehicles are usually approaching on a straight line along the road without lateral deviation. Therefore, a driver would either decelerate, keep the velocity or accelerate along a road, without turning the steering wheel much. Thus, the kinematic values, which need to be examined are reduced to the **position** (and its time derivatives **velocity** and **acceleration**) along the straight line and the vehicle's **pitch**.

As the driver in the vehicle can be seen from outside, he/she too can communicate implicitly, e.g. via looking at the pedestrian. As AV passengers are relieved of the driving task and object and event detection and response (SAE, 2018), there might not be a driver present. Therefore, a relevant question is, whether the **presence of a driver** or his/her **attentiveness** influences the decision making of crossing pedestrians. It was theorized that the type of vehicle might also have an effect on pedestrians decision making when crossing a road – a dark blue mini-van might be perceived as more family friendly and cooperative in comparison to a red sports car.

3.1.2 Explicit communication

Explicit communication is defined in chapter 2 as signalling either perception or movement, without directly achieving those. This can be understood as any mean of communication that is decoupled from the vehicle's movement and commonly understood as actual communication in traffic.

A vehicle can communicate explicitly using its **light interfaces**, such as turn indicators, headlights and braking lights. In lower distances, drivers can explicitly communicate using body language, such as **gestures**.

If a driver is not present or inattentive, the AV has no means to communicate explicitly with other road users, other than the available exterior lights, which usage is defined in traffic regulations. An **eHMI** might be useful as an additional communication interface for AVs to resolve potential deadlock situations. Furthermore, the AV could also project its intention or sensor perception to the outside, thus decreasing decision making times of surrounding traffic (see D4.1 and D4.2 for a detailed description of the interACT interaction strategies).

Figure 8 shows a simplified depiction of the ways a vehicle can communicate with a other road users, which are translated into independent variables for the VR experiments with pedestrians below.

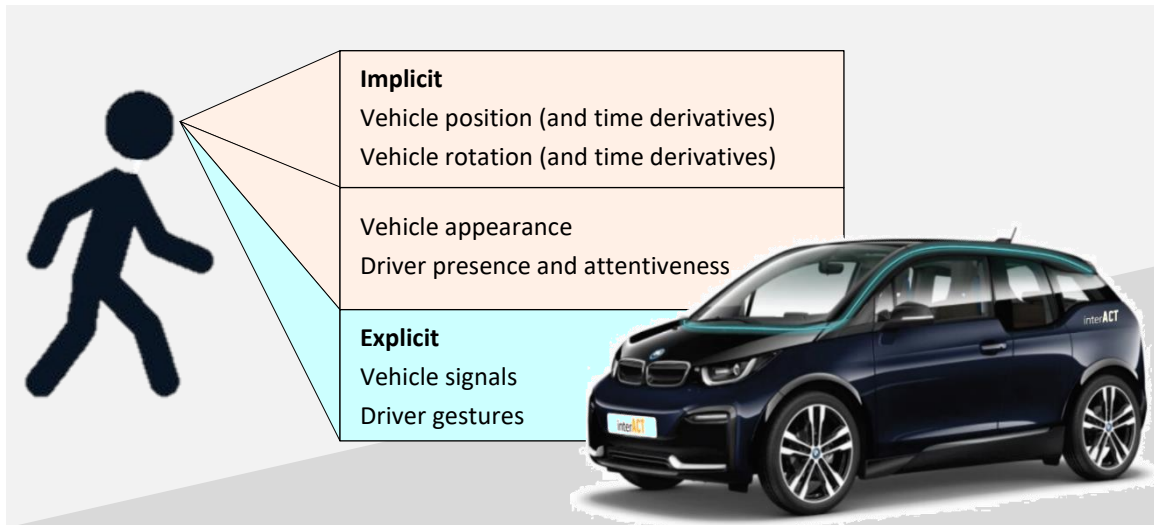


Figure 8: Simplified depiction of visual communication capabilities from vehicles towards other road users

3.2 Results from controlled experiments in VR simulators

3.2.1 Effects of Deceleration Strategy and Jerk on Pedestrian Crossing Behaviour (Dietrich et al., 2019)

Drivers have multiple ways to yield their right of way to a pedestrian with a crossing intention. Once the driver has made his/her decision, the aim is to decelerate the vehicle coming to a full stop short of the pedestrian. Assuming that a driver initiates the deceleration once the yielding decision was made, three possible deceleration strategies were identified, with an equal maximum deceleration value, but different jerks:

- **Defensive:** The driver could initially brake hard to implicitly communicate his/her yielding intent, followed by a slow approach with softer deceleration to the full stop position
- **Baseline:** In this condition, the vehicle is decelerating as constant as possible, raising the deceleration to the maximum value within a second in the beginning and lowering it within a second towards the full standstill
- **Aggressive:** As time is of the essence, the driver might decelerate slowly in the beginning and strongly close to the full stop position. This strategy is somewhat reversed to the defensive strategy, but takes less time to execute

To identify the best strategy, a pedestrian simulator study was conducted with 30 participants. As the virtual simulation enabled the manipulation of vehicle dynamics, the effects of vehicle pitch on pedestrian crossing behaviour was also evaluated. Four pitch conditions were introduced to study, whether an artificial pitch can be utilized as implicit communication in future AVs:

- Normal pitch – realistic vehicle behaviour
- No pitch – the vehicle decelerated without pitching forward
- Boosted pitch – an artificially amplified pitch
- Premature pitch – the vehicle started pitching prior to decelerating

Virtual convoys of vehicles were passing the study participant with 30 km/h. One vehicle within the convoy started to decelerate using one of the three strategies and one of the four pitch conditions. The distance, in which the vehicles started to decelerate was set to 21.5m; the deceleration values can be found in Table 2. Mixed with four gap acceptance scenarios and three repetitions, each participant completed 48 road crossings.

Table 2: Deceleration strategies evaluated in the VR study (see Dietrich et al. 2019)

Strategy	Initial Jerk (m/s ³)	Maximum Deceleration (m/s ²)	Final Jerk (m/s ³)
Baseline	-2	-2	2
Defensive	-4	-2	0.4
Aggressive	-1.17	-2	4

The results show, that the effects of deceleration strategy ($F(1.35, 39.27) = 995.56, p < .001, \eta_p^2 = .97$) and pitch ($F(2.21, 63.96) = 9.87, p < .001, \eta_p^2 = .25$) on the crossing initiation time relative to the vehicle stopping were statistically significant as well as the interaction between these effects ($F(4.41, 0.1) = 2.7, p < .05, \eta_p^2 = .09$). As seen in Figure 9, the defensive strategy lead to a sooner crossing compared to the baseline and aggressive strategy. Due to the hybrid interaction, the main effect pitch could not be interpreted globally, but as Figure 9 shows, the effect was inferior to the deceleration strategy. Furthermore, participants reported to dislike discrepancies between pitching and vehicle behaviour.

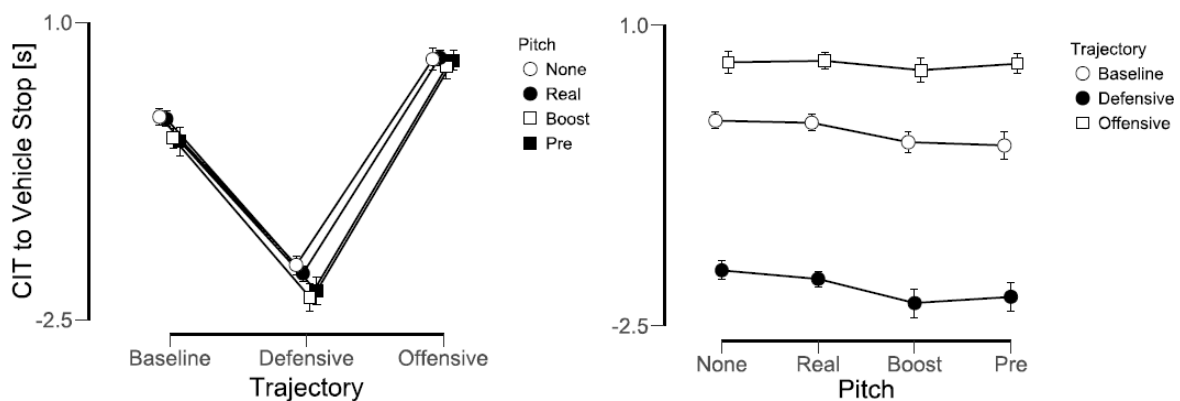


Figure 9: Interaction diagrams of main factors pitch and strategy. (Dietrich et al. 2019)

Overall, pedestrians seem to differentiate different deceleration strategies but mostly through the kinematic movement of the vehicle rather than its dynamics. Therefore, active artificial pitching does not seem to be an appropriate communication method for transmitting yielding intentions in side road velocities.

3.2.2 Effects of Deceleration Distance and Presence of an eHMI on Pedestrian Crossing Behaviour and Perception (Dietrich et al., submitted 2019)

As the deceleration strategy from a fixed distance has a significant effect on the crossing behaviour, the distance itself, from which a vehicle starts to decelerate and thus implicitly communicate the yielding intention, is another factor that could influence pedestrians' decision making. On the one hand, an early deceleration should enable the pedestrian to recognize the yielding intent early, thus speeding up the crossing initiation, on the other hand, a long deceleration distance takes more time than a short one. Furthermore, previous studies have shown (Dietrich et al., 2018) that the presence of an eHMI significantly decreases the crossing initiation. Based on these assumptions, relevant research questions can be formulated:

- How does the deceleration distance influences a pedestrian's crossing?
- What effect does an eHMI have on the crossing initiation of pedestrians and how does this effect interact with the deceleration distance?
- What is the effect of the eHMI on the acceptance of pedestrians?

A VR experiment was conducted to study the effects of deceleration distance and presence of an eHMI on the crossing behaviour of pedestrians. 32 participants were asked to cross a virtual road whenever they felt safe to do so. Analogous to the experiment described in sub-section 3.2.1, a convoy of virtual traffic was presented, with one car decelerating and either displaying the yielding intent with an eHMI resembling the interACT main design (see D4.2, Weber et al. 2019) or not.

Six distances, from which the yielding vehicle would initiate its deceleration, were chosen spanning from 18m to 45m. The deceleration was linearly increased to reach a maximum value within one second, which was hold until the vehicle came to a full stop. This deceleration strategy translates to the deceleration values shown in Table 3.

Table 3: Braking distances and corresponding maximum decelerations evaluated in the VR study (see Dietrich et al., submitted 2019)

Braking Distance [m]	18	24	29	35	40	45
Maximum Deceleration [m/s ²]	-2.5	-1.75	-1.4	-1.13	-.97	-.85

A gap-acceptance condition and a confounding manoeuvre, in which the vehicle decelerated slightly but accelerated again, were added to ensure that participants did not base their crossing decision solely on the eHMI activation or perceivable deceleration.

A Greenhouse-Geisser two way repeated measures ANOVA indicates that both eHMI presence ($F(1, 31) = 33.84, p < .001, \eta_p^2 = .52$) and braking distance ($F(1.64, 50.72) = 180.31, p < .001, \eta_p^2 = .85$) had a significant effect on the crossing initiation time relative to the vehicle coming to a full stop. The interaction between the main effects was not significant ($F(3.92, 121.55) = 2.25, p = .07, \eta_p^2 = .07$). Post hoc pairwise comparisons revealed that pedestrians initiated their crossing sooner, the further away the vehicle was decelerating. An eHMI communicating the yielding intent by a slowly pulsing light of the LED band increased this effect.

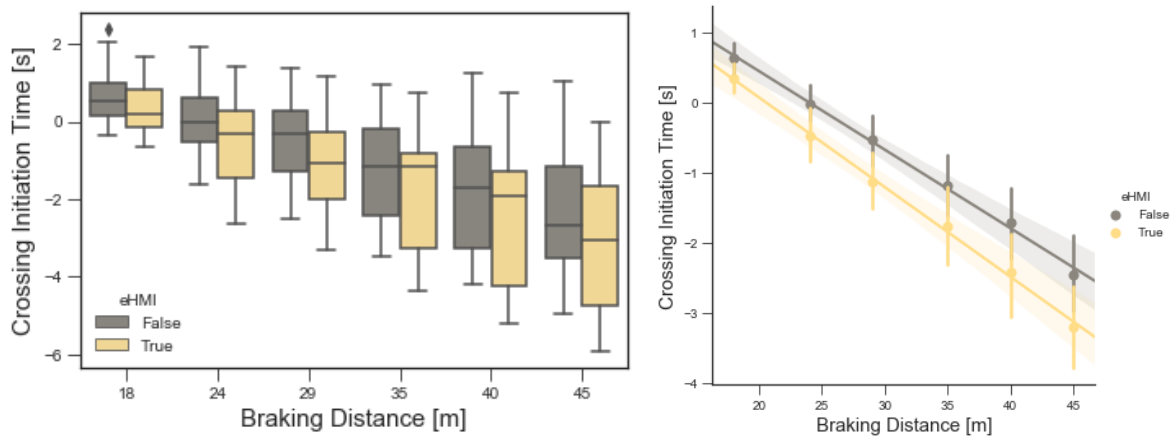


Figure 10: Interaction diagrams of main factors pitch and strategy. (Dietrich et al., submitted 2019)

Figure 10 depicts the connection between braking initiation and crossing initiation of pedestrians as well as the influence of an eHMI being present. Deceleration distance and Crossing Initiation Time show a negative linear correlation (see Dietrich et al., submitted 2019). As seen in Figure 10 on the right, the Crossing Initiation Time was always lower when an eHMI was active. This effect also seems to increase slightly with larger distances.

The presence of an eHMI seems to expedite the decision making process of pedestrians, so that the crossing process is initiated sooner and thus the interaction progressing quicker. Also, decelerating at higher distances leads to pedestrians initiating their crossing way before the vehicle comes to a full stop (negative values on the y-axis). However, as the vehicle is progressing more slowly, the actual time gain is diminished. Further studies should explore, whether the combination of defensive deceleration (see sub-section 3.1.1) in combination with an early braking onset leads to even faster

crossing initiations. The pedestrian also might be outside of the encroachment zone before the vehicle comes to a full stop, thus further increasing the potential of enhancing traffic flow.

3.2.3 Analysis of Gap Acceptances and Effects of Deceleration and Driver Attentiveness on Pedestrian Crossing Behaviour

In order to further explore the outputs of the naturalistic study, an experimental study was conducted to investigate pedestrians' gap acceptance while crossing the road in a virtual environment with a Head-Mounted Display (HMD). In line with UK traffic i.e. driving on the left, two vehicles approached a pedestrian participant from the right hand side and participants were asked to cross (or not) between the two vehicles as they would naturally. The driving behaviour of these vehicles was manipulated, such that the speed of approaching vehicles was either 25mph, 30mph or 35mph (approximately 40, 48 and 56kmh), with a time gaps of between 1 and 8s (increasing in 1 second increments) between the two vehicles. On approach, the second vehicle was either decelerating to come to a stop, or was travelling at constant speed.

Results showed that the mean accepted time gap for non-decelerating trials was 4.6 seconds for 25mph, 4.3 seconds for 30mph, and 4 seconds for 35mph (Lee et al., in prep). Results also shown that the crossing rate was 100% when the second approaching vehicle decelerated and stopped, as opposed to only 52% when the vehicle was not decelerating (Lee et al., in prep). In addition, among these deceleration trials, only 18% of crossings happened while the vehicle was decelerating (between 32.5 m and 2.5 m away), where 51% had already crossed before the deceleration began and 31% crossed after the car had stopped (Lee et al., 2019). There was an effect of speeds on crossing made during deceleration, whereby fewer crossings were made with higher travelling speed (Lee et al., 2019).

Using a similar approach and study design, Velasco et al. (2019) investigated the effect of drivers' attentiveness and presence on pedestrians' crossing decisions and behaviour. Approaching vehicles were travelling at a speed of 20mph with a manipulated time gap of either 3.5 seconds or 5.5 seconds between vehicles. The vehicles either decelerated and stopped or travelled at a constant speed. Three driver conditions were included for the second approaching vehicle, whereby the vehicle was either driverless, or the driver was paying attention to the road (looking straight ahead), or being inattentive (looking at a hand held phone with head tilted towards the right hand side). Participants were asked to cross (or not) naturally between the approaching vehicles. Preliminary findings showed a discrepancy between observed crossing behaviour and reported perceived safety and behavioural control. The attentiveness of drivers did not affect crossing decisions and behaviour, but participants reported higher perceived behavioural control and lower perceived risk while crossing in front of attentive drivers as compared to driverless and inattentive drivers.

These studies used VR to explore the crossing decisions and behaviour of pedestrians while facing vehicles with different time gaps, speeds and deceleration profile. The results show that the crossing decisions and behaviours found using VR are in line with those found on test tracks, making it a useful tool for exploring pedestrians' decision making processes (Lee et al., in prep, 2019). The finding that different speed, deceleration, and time-gap parameters lead to different crossing decisions provides some initial insights into where eHMI might be more likely to have an impact on pedestrians' crossing behaviour and decision making e.g. during the deceleration phase. Although the results of Velasco et al. (2019) show that the presence/effect of drivers does not affect objective measures such as pedestrian crossing decision and behaviour, it does affect their perceived risk and perceived behavioural control. This suggests the importance of understanding pedestrians' feelings while interacting with AVs and provides evidence that eHMI might help with acceptance and trust in automation. This will be explored further as part of WP6 of the interACT project.

3.3 Visual perception and its effect on interaction in traffic

Based on the described studies in section 3.2, the following assumptions can be formulated:

- An early deceleration of the yielding vehicle leads to earlier crossings of pedestrians. This is consistent with the observation studies, where traffic participants adapted their behaviour early, to avoid right of way negotiations and complete stand stills.
- A defensive deceleration, i.e. initially braking more than needed to come to a full stop at the encroachment zone, leads to earlier crossing initiations of pedestrians.
- The presence or attentiveness of a driver does not seem to be a big factor for the crossing decision of pedestrians but affects their perceived safety and perceived control.
- Utilizing eHMIs consistently reduces the time pedestrians need to initiate their crossing. This indicates, that a yielding intent is perceived quicker and more reliably, if the deceleration is combined with an explicit communication.
- The pitch of a vehicle seems to have little effect on the perception of the car's deceleration by other road users. Therefore, active pitching to implicitly communicate a yielding intent is not recommended, especially since it might affect the comfort of AV passengers.

While the studies were focussing on pedestrian-AV interactions from the pedestrian's point of view, the assumptions are likely to be extendable to vehicle-vehicle interactions as well, as the visual perception of an approaching AV are comparable.

4. Quantitative modelling of human-automation interaction

One of the goals of interACT WP2 is to develop quantitative models of human road user behaviour, for example to permit *virtual testing* simulations as part of an AV development and evaluation process. In interACT Deliverable D2.1 these objectives were described in some detail, and the project's first efforts along these lines were described. Specifically, a modelling framework was proposed, describing road user decision-making as an interconnected set of parallel “drift diffusion” (or “evidence accumulation”) decision-making units, driven by time-varying sensory inputs. It was demonstrated how this type of variable-drift diffusion model (VDDM) framework was able to capture qualitative findings from experiments on pedestrian crossing behaviour.

In this chapter, the next stage of work on these models in interACT is described. A set of data collection experiments, specifically designed to support comparison and parameterisation of model alternatives, have been carried out. These experiments addressed the originally considered pedestrian crossing scenario, and also extended the modelling scope to a scenario where a driver turns across oncoming traffic. Data were collected both in the UK and in Japan, in collaboration with Keio University, as part of a twinning activity between interACT and the Japanese project sip-ADUS. Considerable effort was also spent on identifying appropriate methods for fitting these complex models to the empirically observed human behaviour, and part of the outcome of this exercise was the formulation of a simpler type of model.

The final models and simulations have been packaged in a standalone software package, provided with this deliverable. This software can be used to investigate the impact of different AV approaching/yielding behaviours in pedestrian crossing and vehicle turning scenarios. Such use of these models and simulations is one of the objectives of interACT WP6.

The first section below describes the objectives and research questions guiding the work, and is followed by a section describing the data collection experiments carried out, and the models that were developed and tested. The third section presents and discusses the obtained results, and the fourth section provides conclusions in the form of answers to the stated research questions. Two final sections describe the model simulation software provided as an addendum to this report, and planned and possible directions for future work.

4.1 Objectives and research questions

The primary objective of the work described in this chapter was to:

Develop models that predict the timing of pedestrian crossing and vehicle turning decisions as a function of the behaviour of an approaching (automated) vehicle, and

provide these models in a form such that they can be used in virtual development and testing of AVs.

A secondary objective was to investigate what determines subjectively perceived feelings of safety while crossing a road.

To address these objectives, a number of more specific research questions were formulated:

- RQ1: Can the originally proposed VDDM framework capture the human behaviour in the studied crossing/turning scenarios?
- RQ2: Can the models be scaled down to less complex versions?
- RQ3: Can the same basic type of model be used both for pedestrian crossing and driver turning decision-making?
- RQ4: Can the same basic type of model be used both for UK and Japanese road users, and if yes do the models need to be parameterised differently?
- RQ5: To capture effects of available gap on crossing/turning behaviour, is it enough to consider only time to arrival, or should distance cues also be considered?
- RQ6: To capture effects of vehicle deceleration on crossing/turning behaviour, is it enough to consider only time and/or distance gaps, or are direct cues describing deceleration also needed?
- RQ7: Are there correlations between the kinematical conditions at crossing/turning and subjective ratings of perceived safety?

4.2 Methods

4.2.1 Data collection

Briefly stated, the data collection experiments had participants wear a VR headset to experience a number of variations of either a pedestrian crossing or a driver turning scenario, and to signal their crossing/turning decisions in each scenario trial by pressing a button. After each trial, participants also provided subjective feedback on how they experienced the trial.

The data collections were approved by the relevant research ethics committees at the University of Leeds and Keio University.

Overall experiment design and participants

As illustrated in Table 4, the complete collected data set involved a total of 80 participants, split into four groups by the two between-participant factors *Traffic scenario* (*pedestrian crossing* and *driver turning*) and *Country* (*UK* and *Japan*). The table also provides the participant demographic information for each group.

Table 4: Overall experiment design and participant demographics for the data collection carried out to support model development.

		Country	
		UK	Japan
Traffic scenario	Pedestrian crossing	20 participants (10 male; ages 20-60, median 25)	20 participants (11 male; ages 19-33, median 21.5)
	Driver turning	20 participants (9 male; ages 19-42, median 27)	20 participants (11 male; ages 18-34, median 22)

The UK participants were recruited via a University of Leeds participant pool. The Japanese participants were recruited via a temporary employment agency.

Procedure and materials

Upon arrival, participants provided informed consent and their demographic data. They were instructed that they would be wearing a VR headset (this was a HTC Vive head-mounted display, with virtual scenes created in Unity 2018), and that they would use one of the buttons on the handheld VR controller to progress through the experiment. They were told that they would experience a number of repetitions of the same basic traffic scenario, where their task was to first turn their head to look for approaching traffic, then press the controller button to walk/drive across the road when they judged that it was safe to do so, and then finally provide subjective feedback on the experience. More specifically, each scenario trial proceeded according to the following sequence:

First, participants were shown a blank screen, with an instruction on where to orient their head (straight ahead in the pedestrian crossing scenario, to the right in the driver turning scenario); this text message was located in the intended head orientation location. Upon pressing the controller button, the VR scene was changed to a virtual traffic scene (described in detail in the next section), where the participant’s head orientation meant that they were in both scenarios looking across the road to be crossed, rather than at any approaching traffic on that road. Participants then turned their head to look for the approaching traffic, and, unbeknownst to the participants, this triggered the instantiation of an approaching vehicle. When the participant pressed the button to indicate their decision to cross/turn, the position of the VR “camera” was moved across the road, emulating walking/driving. From here onward, this decision will for simplicity be referred to as the crossing decision, for both scenarios.

The use of a button press to initiate movement, rather than having participants physically walk or use pedals/steering wheel, was adopted for maximum experimental control, minimum time overhead, and also to make the two traffic scenarios maximally comparable. Once participants reached the other

side of the road being crossed, the virtual traffic scene was again replaced by the blank scene, now showing two subjective rating items:

1. The vehicle yielded to me.
2. It was safe to cross before the vehicle.

The participants indicated verbally to the experimenter their agreement with these two statements, in both cases using the following 5-point Likert scale, also displayed in the virtual scene:

1: Strongly disagree, 2: Disagree, 3: Somewhat agree, 4: Agree, 5: Strongly agree

Pressing the controller button again, initiated the next trial, starting with the instruction on where to orient their head.

For the data collection in Japan, Japanese versions of the instructions to participants and the subjective rating items and scales were checked by a person fluent in both English and Japanese, external to the project team but with subject-matter expertise in the area.

The pedestrian crossing scenario

In the pedestrian crossing scenario, the VR scene was the one shown in Figure 11, with the participant positioned next to a straight, two-lane road of width 5.85 m, initially looking straight across a zebra crossing. When the participant turned their head to the right to look for traffic in the nearest lane (both UK and Japan have left hand drive traffic), this triggered the instantiation of an approaching vehicle, appearing at an initial distance D_{init} with initial speed v_{init} , i.e., with initial time to arrival $TTA_{init} = D_{init}/v_{init}$.



Figure 11: The VR scene in the pedestrian crossing scenario.

The two insets show a birds-eye-view (not seen by the participants), as well as the view across the zebra crossing at the start of each scenario.

In each trial experienced by the participant, the movement of the approaching vehicle was different. There was a total of 16 such *Scenario variants*, across three *Scenario types*: *Constant velocity*, *Decelerate to a stop*, and *Decelerate without stopping*.

Parameter details for the 16 scenario variants are provided in Table 5 below. In the six *Constant velocity* scenario variants, the approaching vehicle maintained the initial speed v_{init} throughout the scenario. In the eight *Decelerate to a stop* scenario variants, the vehicle decelerated from the start of the scenario, with a constant deceleration so as to reach zero speed at a distance D_{stop} . In the two *Decelerate without stopping* variants, the vehicle also decelerated from the start of the scenario, but the constant deceleration rate was instead chosen so as to reach a final speed of $v_{final} = 5$ km/h at distance D_{stop} , after which point the vehicle continued past the pedestrian crossing at speed v_{final} .

Table 5: Pedestrian crossing scenario variants.

Scenario type	v_{init} (km/h)	D_{init} (m)	TTA_{init} (s)	D_{stop} (m)
Constant velocity	25	15.90	2.29	N/A
	50	31.81	2.29	N/A
	25	31.81	4.58	N/A
	50	63.61	4.58	N/A
	25	47.71	6.87	N/A
	50	95.42	6.87	N/A
Decelerate to a stop	25	15.90	2.29	4
	50	31.81	2.29	4
	50	31.81	2.29	8
	25	31.81	4.58	4
	50	63.61	4.58	4
	50	63.61	4.58	8
	25	47.71	6.87	4
	50	95.42	6.87	4
Decelerate without stopping	50	27.78	2	8
	50	41.67	3	8

These scenarios were defined so as to allow testing of models across a broad range of vehicle approach kinematics, including different speeds and different TTAs, but also with different D_{stop} distances for the same TTAs, to allow stringent testing of RQ5. The use of two different values for D_{stop} was used to study effects of deceleration rate on behaviour, with reference to RQ6. The specific scenario parameters were identified based on simulations using the provisional model described in (Dietrich et al., 2018; Markkula et al., 2018), to identify a set of scenario variants that was likely to result in predominantly early crossing decisions for some variants (e.g., the $TTA = 6.87$ s variants),

predominantly late crossing decisions for some variants (e.g., the TTA = 2.29 s scenarios), and a mix of both early and late decisions for the remaining variants. The motivation for the *Decelerate without stopping* scenario type was to introduce some ambiguity with respect to deceleration, to reduce learning effects where the participant might come to expect that any deceleration was guaranteed to be a deceleration to yield to them.

When the participant pressed the designated controller button, the VR camera position was translated across the road at 1.31 m/s (in the range of typical speeds for walking and crossing roads; Montufar et al., 2007), but the participant could still control the camera orientation with their head, just as before, e.g., to look at the approaching car while crossing.

The driver turning scenario

The driver turning scenario was similar in its setup to the pedestrian crossing scenario. Here, only the main differences between the two scenarios are described.

In this scenario, as illustrated in Figure 12, the virtual traffic scene had the participant in the driver's seat of a passenger car, initially positioned at a slight angle in an intersection, approximately 8.5 m longitudinally from the centre line of the crossing lane into which the participant was to turn. The initial head orientation of the participant was to the right, in the intended direction of travel. In this scenario, this initial head orientation was further supported by a fixation object in the VR scene (the blue square in the rightmost inset in Figure 12), and the approaching vehicle was instantiated once the participant turned their head to the left.



Figure 12: The VR scene in the driver turning scenario. The two insets show a birds-eye-view (not seen by the participants), as well as the view across the intersection at the start of each scenario.

The same three scenario types as in the pedestrian crossing were used, but with different parameter values, to account for the different nature of the task. As can be seen in Table 6, higher TTA_{init} values were used, since crossing the road took longer time to in this scenario than in the pedestrian scenario. The D_{stop} values were also larger, to have the approaching vehicle stop before entering the intersection rather than just in front of the participant’s vehicle.

When the participant pressed the designated controller button, the participant’s car, and the VR camera position within accelerated at 2 m/s^2 along a right-turn trajectory onto the crossing road, passing the middle of the approaching car’s lane after 2.7 s.

Table 6: Driver turning scenario variants.

Scenario type	v_{init} (km/h)	D_{init} (m)	TTA_{init} (s)	D_{stop} (m)
Constant velocity	25	20.83	3	N/A
	50	41.67	3	N/A
	25	41.67	6	N/A
	50	83.33	6	N/A
	25	45.14	6.5	N/A
	50	90.28	6.5	N/A
Decelerate to a stop	25	27.78	4	22.18
	50	55.56	4	22.18
	50	97.22	7	26.18
	25	48.61	7	22.18
	50	83.33	6	22.18
	50	76.39	5.5	26.18
	25	38.19	5.5	22.18
	50	69.44	5	22.18
Decelerate without stopping	50	83.33	6	22.18
	50	69.44	5	22.18

4.2.2 Models

Some of the research questions defined in this chapter were addressed by means of inferential statistical testing, but the bulk of the data analysis was done in the form of development and testing of two types of models.

Variable-drift diffusion models (VDDMs)

The first type of model was derived from the general framework described by Markkula et al. (2018). This framework starts from the basic building block of a drift diffusion model (DDM), which models

two-choice decision tasks as a biased random walk towards two opposing decision thresholds (see, e.g., Ratcliff et al., 2016, for an overview), and extends it in the first instance by allowing time-varying inputs. For this reason, these models will be referred to here as variable-drift diffusion models (VDDMs). Markkula et al. (2018) further extended this type of model by suggesting that several of these decision units can be interconnected. The leftmost panel in Figure 13 shows the pedestrian crossing model proposed in the original paper, referred to here as the “connected VDDM” (C-VDDM), because it models the action decision as dependent on two purely perceptual decisions, to which it is connected. The other two panels show simplified versions of this model, the dual VDDM (D-VDDM) and the single VDDM (S-VDDM). In this figure, each coloured square is a DDM unit, τ is the visually perceived TTA (or time to collision TTC, loosely speaking) of the vehicle (Lee, 1976), $\dot{\tau}$ is the rate of change of this quantity, k_1 and k_2 are model parameters, and CT is the crossing time, predicted to occur by the model as the DDM for “I am crossing now” crosses a positive threshold. Full implementation details are not provided here; please refer to (Markkula et al., 2018; Giles et al., 2019).

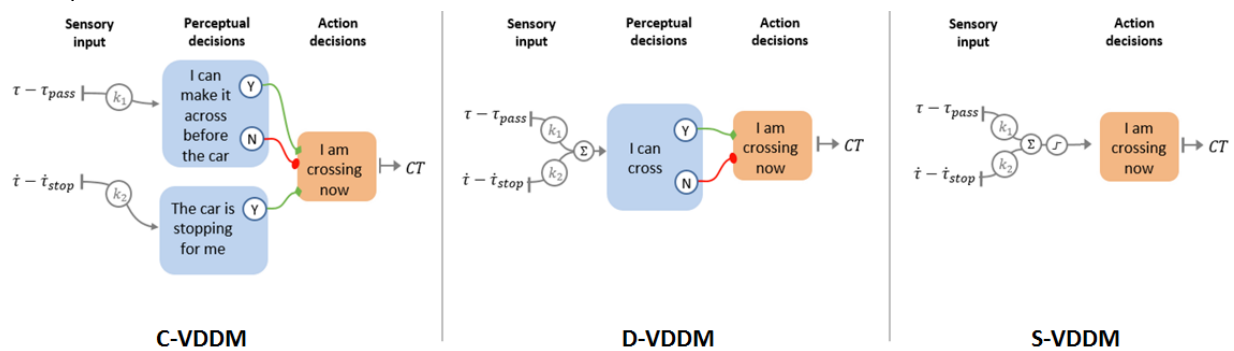


Figure 13: Illustration of the three model types tested here.

To fit these models to the obtained data, a pseudo-likelihood maximisation approach was used. A particle swarm optimisation (PSO) algorithm (Wahde, 2008) with 50 particles, running for 50 iterations, was used to search the model parameter space. At each model parameterisation visited by the PSO algorithm, 5000 model simulations were run for each scenario variant, to obtain a numerical approximation of the probability distribution of CT in each trial, and the model likelihood was then obtained as the product of the probabilities of the experimentally observed crossing times, according to these numerically estimated probability distributions. A limitation with this approach is that, due to the limited number of simulations, the numerically estimated probability distribution can sometimes be zero in some regions, even if the true probability distribution for the model wouldn't be. In some cases, this was found to push the model fitting towards excessively high noise amplitudes, yielding model behaviour that was clearly not representing the human data well. Therefore, the distribution estimated from the model was mixed with a uniform “slack” distribution, with weight $P_{slack} = 0.02$

for the uniform distribution. This made almost no discernible difference to the overall estimated distribution, but got around the problem of excessively noisy model fits.

The model parameters were:

- τ_{pass} : τ value above which the model tends to judge that it is possible to cross in front of the approaching vehicle; fixed at the actual crossing times 2.46 s and 3.46 s, respectively, for the pedestrian crossing and driver turning scenarios.
- \hat{t}_{stop} : \hat{t} value above which the model tends to judge that the approaching vehicle is decelerating to stop in front of the crossing road user; fixed at -0.5 (see Lee, 1976).
- T : evidence accumulation decay constant
- $\mathbf{K} = [k_1, k_2]$: vector of input gains
- \mathbf{Y} : vector of connection weights from “yes” output nodes
- \mathbf{N} : vector of connection weights from “no” output nodes
- $\boldsymbol{\sigma}$: vector of evidence accumulation noise standard deviations
- η : input saturation threshold (S-VDDM model only)

For the C-VDDM and D-VDDM, two variants were fitted; one model variant where all evidence accumulation units had separate noise standard deviations (vector $\boldsymbol{\sigma}$), and one model variant where a single noise standard deviation was shared across all evidence accumulation units in the model (scalar σ).

Threshold distribution models (TDMs)

As with any complex, many-parameter model, parameter-fitting of the VDDMs is not trivial. As will be further illustrated below, the adopted PSO approach, although more successful than other attempted methods, showed indications of getting stuck in local optima. Furthermore, regardless of fitting method, the VDDM parameters have a degree of redundancy (e.g., a high input gain to one accumulator can be compensated by a low input gain to another, and vice versa), which makes it difficult to interpret obtained parameter values.

For these reasons, a second, simpler type of model was also devised, which will here be referred to as threshold distribution models (TDMs). To begin with, these TDMs were made maximally simple by modelling the crossing decision solely based on τ , since the VDDM fits suggested that this variable alone could to a large extent account for the observed human decisions in both scenarios. This TDM assumed two probability distributions:

1. One probability distribution for τ_{pass} , the τ threshold above which an individual will accept crossing in front of the approaching vehicle.
2. One probability distribution for a reaction time T_R , from the threshold-passing $\tau > \tau_{pass}$ until the crossing decision (the button press, in this study).

To generate a distribution of crossing times from this model for each scenario variant, the τ signal in the scenario variant is traced from the start, and as soon as a new portion of the τ_{pass} distribution is covered for the first time, an instance of the T_R distribution is added to the crossing time distribution, starting from the scenario time step in question, and with probability mass equal to the fraction of the τ_{pass} distribution that was covered in that time step. Another way of describing it is that at each scenario time step, a Dirac delta is generated of amplitude equal to the portion of the τ_{pass} distribution that was encountered for the first time in that time step, and the final crossing time distribution is then obtained as the convolution of this train of Dirac delta spikes with the T_R distribution. Figure 14 provides an illustration, referring to the train of Dirac delta spikes as a “decision time density”.

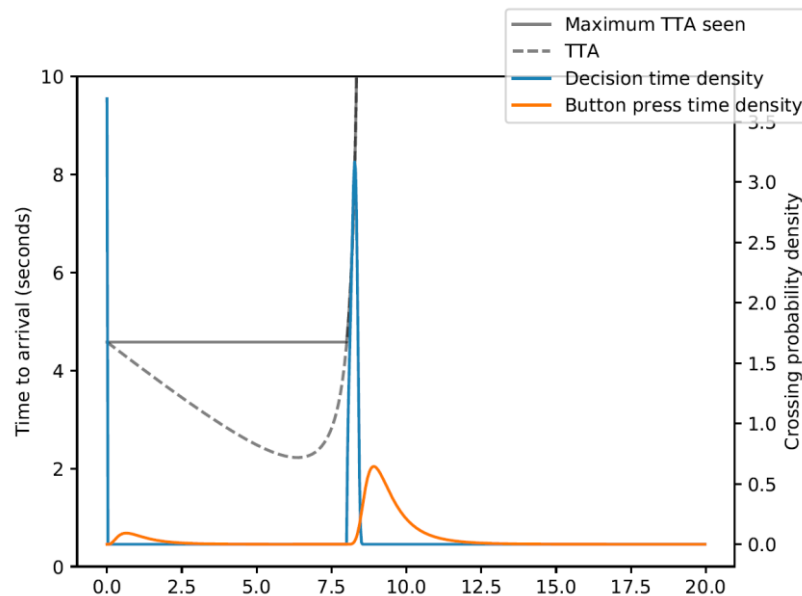


Figure 14: Illustration of the threshold distribution model (TDM) in a scenario with an approaching vehicle.

The vehicle appears at 4.6 s initial TTA (τ) and decelerates to come to a full stop about 8 s into the scenario (x-axis shows time in seconds). The initial TTA triggers a first spike in a “decision time” distribution, and the rest of that distribution, up to total mass of 1, is then added later in the scenario as the (apparent, deceleration-independent) TTA rises above the initial TTA. The decision time density is then convolved with a reaction time distribution to yield the final crossing time (button press) distribution. See the text for a full description.

Similarly to the VDDMs, the TDMs were fitted by means of likelihood maximisation, but due to the closed form of the model the TDM likelihood calculations were exact rather than pseudo-likelihoods. The maximisation was done using the Basinhopping global optimisation method (Wales and Doye, 1997) as implemented in Scipy version 1.1.0 (Jones et al., 2019). The Basinhopping was run for 100 iterations using Powell's conjugate direction method (Powell, 1964) as the local optimizer as implemented in Scipy 1.1.0. As the objective function is not convex, also in this case it is not certain

that global optima were reached, however analysis of the results and produced parameterisations do indicate reasonable fits.

Once it had been established that this type of model and fitting approach were successful, more elaborate TDM variants were also tested. These models replaced the τ threshold distribution with a threshold distribution for a more general quantity $\tilde{\tau}$, to investigate also distance and acceleration effects. In its most complex form, this quantity was formulated as follows:

$$\tilde{\tau} = \frac{d^p}{v^q} + k(\dot{t} + 1)$$

The first term on the right hand side is a generalised TTA, inspired by the well-known Gazis-Herman-Rothery model of car-following (Gazis et al, 1961; Brackstone and McDonald, 1999). Note that with $p = q = 1$ this term reduces to τ . The second term is the deceleration term, similar to how it was included in the VDDMs, but with $\dot{t}_{stop} = -1$ instead of $\dot{t}_{stop} = -0.5$. From a model behaviour perspective, this difference is just a matter of notation, since the TDM can be rewritten so as to absorb this constant into the overall distribution $\tilde{\tau}_{pass}$ (the $\tilde{\tau}$ threshold above which an individual will accept crossing in front of the approaching vehicle).

The full list of model parameters was:

- m_{pass} : exponential of the mean of the associated normal distribution for the lognormal $\tilde{\tau}_{pass}$ distribution.
- s_{pass} : standard deviation of the associated normal distribution for the lognormal $\tilde{\tau}_{pass}$ distribution.
- m_R : exponential of the mean of the associated normal distribution for the lognormal T_R distribution.
- s_R : standard deviation of the associated normal distribution for the lognormal T_R distribution.
- p : distance exponent in the generalised TTA.
- q : speed exponent in the generalised TTA.
- k : gain for the deceleration term.
- $\tilde{\tau}_{passed}$: a $\tilde{\tau}$ threshold below which the approaching road user is considered to effectively have passed the crossing road user (especially relevant for the driver turning scenario, where it takes a non-negligible time for the crossing road user to move into the conflict area after initiating crossing; in the VDDMs this time was explicitly included as a constant, set to the actual value of this movement time).
- P_{slack} : weighting for the uniform slack distribution (as for the VDDMs).

Since the TDM fitting procedure was computationally efficient, an exhaustive model fit analysis was carried out to investigate which of these parameters to include in the final model. In this analysis, all possible combinations were tested of keeping each parameter free or fixed (at a value excluding the

parameter in question from the model, e.g. $k = 0$), with the exception of the four distribution parameters and \tilde{t}_{passed} , which were always included as free parameters.

4.3 Results and discussion

4.3.1 Model fits for the variable-drift diffusion models

Below, tables and figures are provided detailing the results of the various VDDM model fits. In the tables, # denotes model parameter count, $\log(L)$ is pseudo log-likelihood as described above, with higher (smaller negative) values indicating better model fit, the AIC is the Akaike Information Criterion (Akaike, 1974), a goodness-of-fit quantity adjusting for model parameter count, with smaller values indicating more preferable models. In the tables, the symbol † indicates a parameter value at a bound of the PSO search range, which may suggest that a better fit would be attainable by expanding the search space, and in some cases this may also suggest that the obtained model fit is not aligning well with the theory behind the model (e.g., deleting a hypothesised connection between decision units by setting it to zero). Models with at least one such at-bound parameter value are shown in orange font. The preferable model according to the goodness-of-fit metrics is indicated in bold face, and if that model had one or more parameter values at search range bounds, also the preferable model without any such parameter values is indicated in bold face.

Pedestrian crossing scenario

Table 7: VDDM fits for the UK pedestrian crossing scenario. See the text for meanings of symbols and formatting.

Model	#	$\log(L)$	AIC	T	K	Y	N	σ	η
C-VDDM	9	-874.1	1766.3	0.21	[2.91, 0.5]	[2.83, 0.79]	[0.7]	[0.99, 1.99, 0.92]	N/A
C-VDDM1s	7	-953.7	1921.4	0.67	[4.35, 0.46]	[0.44, 1.83]	[0.76]	[0.87]	N/A
D-VDDM	7	-924.7	1863.3	0.1	[10†, 10†]	[2.73]	[0†]	[0.96, 2.0]	N/A
D-VDDM1s	6	-871.9	1755.8	0.26	[0.66, 0.42]	[3.25]	[10†]	[1.03]	N/A
S-VDDM	5	-882.0	1774.1	0.34	[0.47, 0.19]	N/A	N/A	[1.05]	2.5

Table 8: VDDM fits for the Japanese pedestrian crossing scenario. See the text for meanings of symbols and formatting.

Model	#	$\log(L)$	AIC	T	K	Y	N	σ	η
C-VDDM	9	-923.5	1865.0	1.24	[3.78, 0.18]	[0†, 2.15]	[0.38]	[0.73, 1.63, 0.21]	N/A
C-VDDM1s	7	-978.9	1971.9	0.69	[3.09, 0.29]	[0.22, 1.93]	[0†]	[0.62]	N/A
D-VDDM	7	-908.6	1831.2	0.24	[0.77, 1.28]	[3.51]	[4.93]	[0.83, 2.0]	N/A
D-VDDM1s	6	-922.3	1856.6	0.61	[0†, 0.21]	[2.13]	[2.04]	[0.71]	N/A
S-VDDM	5	-904.2	1818.4	0.87	[0.15, 0.12]	N/A	N/A	[0.73]	1.91

As shown in the tables and figures in this section, the obtained human pedestrian crossing time distributions were non-trivial, with two or even three modes, but the VDDMs managed quite well to reproduce the observed patterns in the datasets from both countries.

For the UK data, the D-VDDM1s variant performed best. This model's "no"-connection weight was fitted to its maximum value within the search space bound, whereas for the D-VDDM variant (with two separate noise values), both input gains were at maximum bound, and the "no"-connection weight was zero. Overall this could be taken to suggest that both two-accumulator VDDM variants had to be fitted in somewhat unintended ways to reproduce the human data. Also, these two fits together provide a clear indication of the tendency of the PSO fitting method to get stuck in local optima: The behaviour of the best-performing D-VDDM1s can be reproduced exactly by the D-VDDM variant, by simply duplicating the single noise parameter across both accumulators, yet the PSO did not find this better parameterisation for the D-VDDM variant. The fits for the other model variants did not reach search range bounds. Among these, the C-VDDM variant performed best, but the considerably simpler S-VDDM variant produced rather similar distributions and goodness-of-fit (compare the blue and green lines in the example figures). Compared to the best-fit D-VDDM1s (purple line in the figures), the slightly worse fits of the C-VDDM and S-VDDM variants seem to be due to a tendency to place too little probability mass at the peaks later in the scenarios.

For the Japanese data, there was somewhat less spread between model variants in the produced probability distributions and goodness-of-fit. Only the D-VDDM and S-VDDM fits were free of at-bound parameter values, and these two were also the best fits overall, with the S-VDDM as the best-performing model.

Comparing between the UK and Japanese datasets and models there are clear indications that the Japanese participants were more careful, generally crossing later in a given scenario than the UK participants. This can be seen in the human crossing times shown in the figures below, and aligns with existing comparisons of Japanese and French pedestrians (Sueur et al., 2013). The fitted model distributions also reflect this pattern, implemented not least in terms of the lower input gain parameter values in K for the Japanese model fits (in practice it is more subtle than just the input gains; also the other parameters matter).

A possible overall conclusion from the pedestrian crossing VDDM fits is that the S-VDDM performs consistently rather well, despite its simplicity compared to the other model variants. It is also clear, however, that the PSO model fitting procedure is far from perfect.

$$TTA_{init} = 4.6 \text{ s}; v_{init} = 25 \text{ km/h}; D_{init} = 32 \text{ m} \quad TTA_{init} = 4.6 \text{ s}; v_{init} = 50 \text{ km/h}; D_{init} = 64 \text{ m}$$

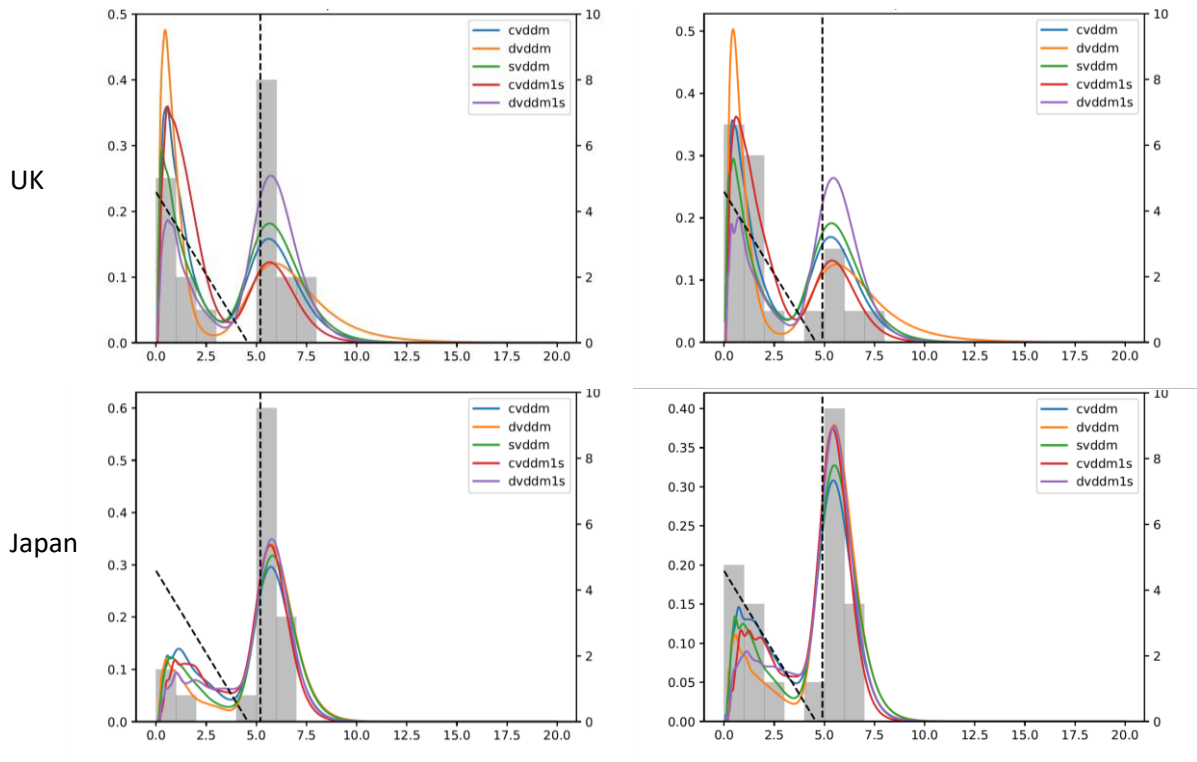


Figure 15: Human pedestrian crossing times (gray bars) and probability distribution predictions by fitted VDDM variants (solid lines), across time elapsed in the scenario (x axis, seconds), in two example *Constant velocity* scenarios with same TTA_{init} but different v_{init} and D_{init} . The dashed lines show TTA during the scenario (right y axis, seconds).

$TTA_{init} = 4.6 \text{ s}; v_{init} = 50 \text{ km/h}; D_{stop} = 4 \text{ m}$

$TTA_{init} = 4.6 \text{ s}; v_{init} = 50 \text{ km/h}; D_{stop} = 8 \text{ m}$

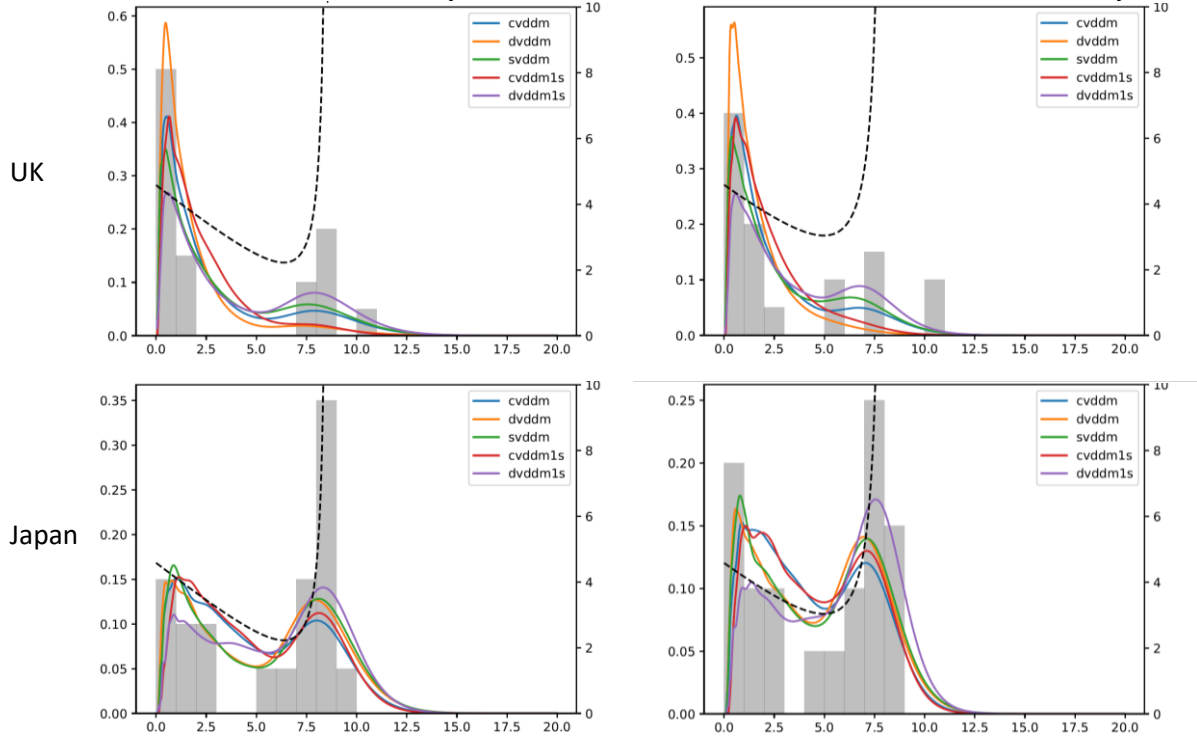


Figure 16: Human pedestrian crossing times (gray bars) and probability distribution predictions by fitted VDDM variants (lines), across time elapsed in the scenario (x axis, seconds), in two example *Decelerate to a stop* scenarios with same TTA_{init} and v_{init} but different D_{stop} . The dashed lines show TTA during the scenario (right y axis, seconds).

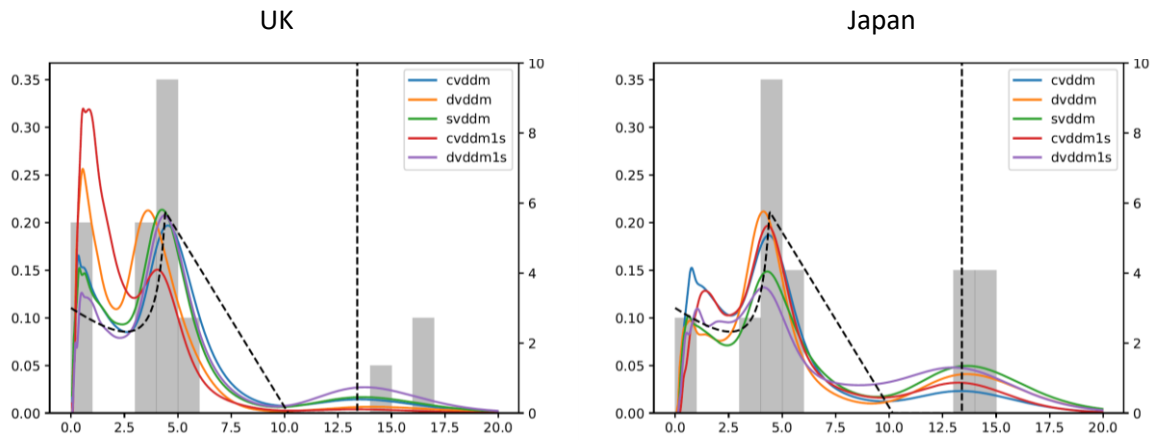


Figure 17: Human pedestrian crossing times (gray bars) and probability distribution predictions by fitted VDDM variants (lines), across time elapsed in the scenario (x axis, seconds), in the *Decelerate without stopping* scenario with $TTA_{init} = 3$ s. The dashed lines show TTA during the scenario (right y axis, seconds).

Driver turning scenario

Table 9: VDDM fits for the UK driver turning scenario. See the text for meanings of symbols and formatting.

Model	#	$\log(L)$	AIC	T	K	Y	N	σ	η
C-VDDM	9	-944.1	1906.2	0.49	[4.46, 0.37]	[0+, 2.11]	[0+]	[0.8, 0.25, 0.59]	N/A
C-VDDM1s	7	-997.4	2008.7	0.32	[3.81, 0.58]	[0+, 2.69]	[0.01]	[0.86]	N/A
D-VDDM	7	-951.3	1916.6	0.04	[0+, 3.0]	[10+]	[8.34]	[1.96, 0+]	N/A
D-VDDM1s	6	-1098.9	2209.8	0.24	[0+, 9.81]	[0+]	[3.42]	[1.56]	N/A
S-VDDM	5	-1118.3	2246.7	0.2	[10+, 10+]	N/A	N/A	[1.32]	0.61

Table 10: VDDM fits for the Japanese driver turning scenario. See the text for meanings of symbols and formatting.

Model	#	$\log(L)$	AIC	T	K	Y	N	σ	η
C-VDDM	9	-894.4	1806.8	0.33	[5.61, 0.52]	[0+, 2.47]	[0+]	[0.74, 0.97, 0.74]	N/A
C-VDDM1s	7	-1064.6	2143.2	0.07	[4.77, 1.25]	[4.08, 4.6]	[4.28]	[1.14]	N/A
D-VDDM	7	-1169.5	2353.0	0.12	[10+, 9.55]	[0+]	[3.98]	[1.72, 0+]	N/A
D-VDDM1s	6	-921.6	1855.1	0.17	[0+, 0.78]	[3.88]	[8.13]	[1.02]	N/A
S-VDDM	5	-900.6	1811.18	0.39	[0+, 0.27]	N/A	N/A	[0.8]	2.26

While in the pedestrian crossing scenario the VDDM distributions generally captured the overall structure of the human crossing time distributions, this was not always the case in the driver turning scenario. The figures below show that the models were in many cases predicting either some probability distribution mode that the humans did not exhibit (e.g., see the green line for the S-VDDM in the top left panel of Figure 18) or lacked a mode that the humans did exhibit (e.g., see the orange

line for the D-VDDM in several panels in all three figures below in this section). Looking at parameter values and goodness-of-fit, the general pattern here was that many model parameters were fit to search range bounds, and the most complex three-accumulator model variants (C-VDDM and C-VDDM1s) performed best, both for the UK and Japanese datasets. Overall, this could be taken to suggest that the VDDMs as currently formulated are missing or incorrectly describing some aspect of the human behaviour in this scenario, causing the fitting to push the models into “strange” parameterisations, a type of situation where the more flexible many-parameter models will naturally be more successful.

One possible aspect of the human behaviour that may be contributing to this situation is what seems to be a distance-dependence in the human crossing decisions. The two scenarios shown in the left and right columns of Figure 18 clearly suggest that the human participants crossed before the passing vehicle more often for the scenario variant with the longer initial distance (right column of panels), even though the initial TTA was the same in both scenarios. A similar but weaker pattern can be seen also for the pedestrian crossing data (Figure 15). There is an existing literature pointing to the importance of distance cues in road-crossing judgments (Davis and Swenson, 2004; Lobjois and Cavallo, 2007; Yannis et al., 2013), and this motivated RQ5 and the design of the scenario variants here. However, the VDDMs as currently formulated did not consider distance effects, making the two scenarios in Figure 18 indistinguishable to the models.

Comparing the UK and Japanese datasets and models, there are again indications of more careful crossing behaviour by the Japanese participants, although possibly less pronounced here than for the pedestrian crossing scenario. Nevertheless, this slight difference may be contributing to the somewhat better fits overall of the VDDMs to the Japanese data; as can be seen in the right column of Figure 18 the Japanese participants did not have the same tendency as the UK participants in this scenario to make an early, distance-based crossing decision, making the human data easier to fit for the distance-blind VDDMs. Under these circumstances, the S-VDDM again performed rather similarly to the more complex models.

Overall, the performance of the VDDMs as currently formulated was not satisfactory for the driver turning scenario, and incorporation of distance cues would seem like one natural direction for model reformulation.

$$TTA_{init} = 6 \text{ s}; v_{init} = 25 \text{ km/h}; D_{init} = 42 \text{ m} \quad TTA_{init} = 6 \text{ s}; v_{init} = 50 \text{ km/h}; D_{init} = 83 \text{ m}$$

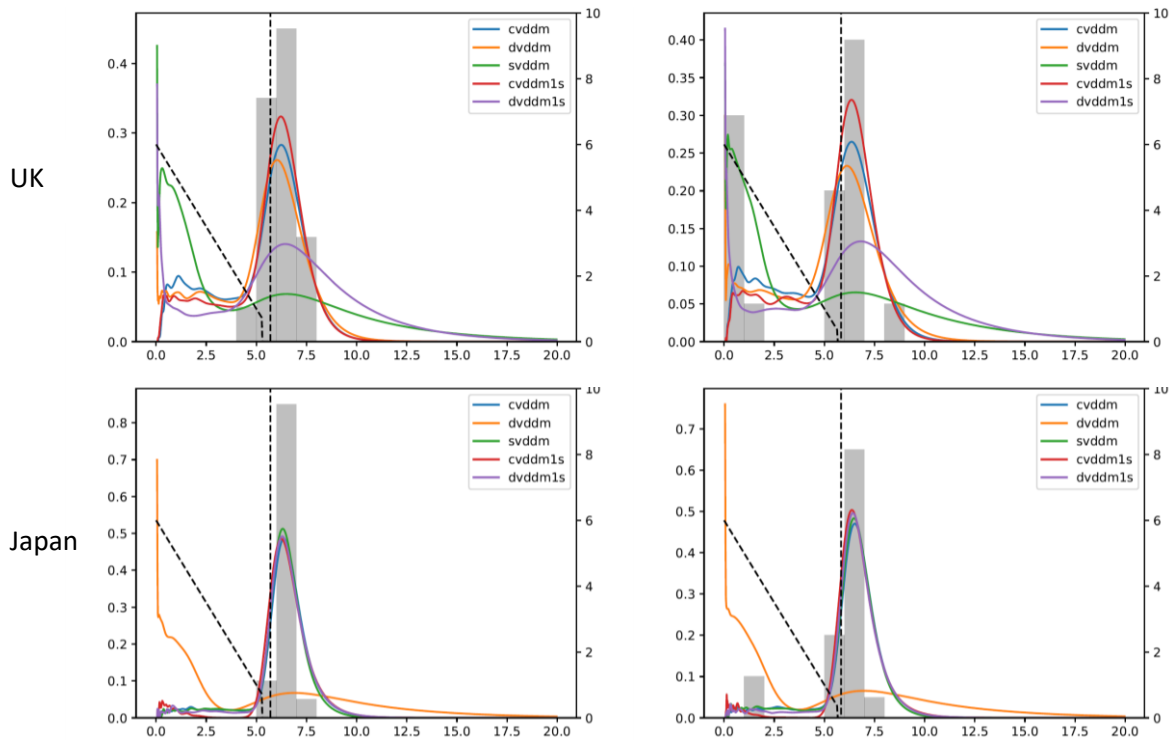


Figure 18: Human driver turning times (gray bars) and probability distribution predictions by fitted VDDM variants (solid lines), across time elapsed in the scenario (x axis, seconds), in two example *Constant velocity* scenarios with same TTA_{init} but different v_{init} and D_{init} . The dashed lines show TTA during the scenario (right y axis, seconds).

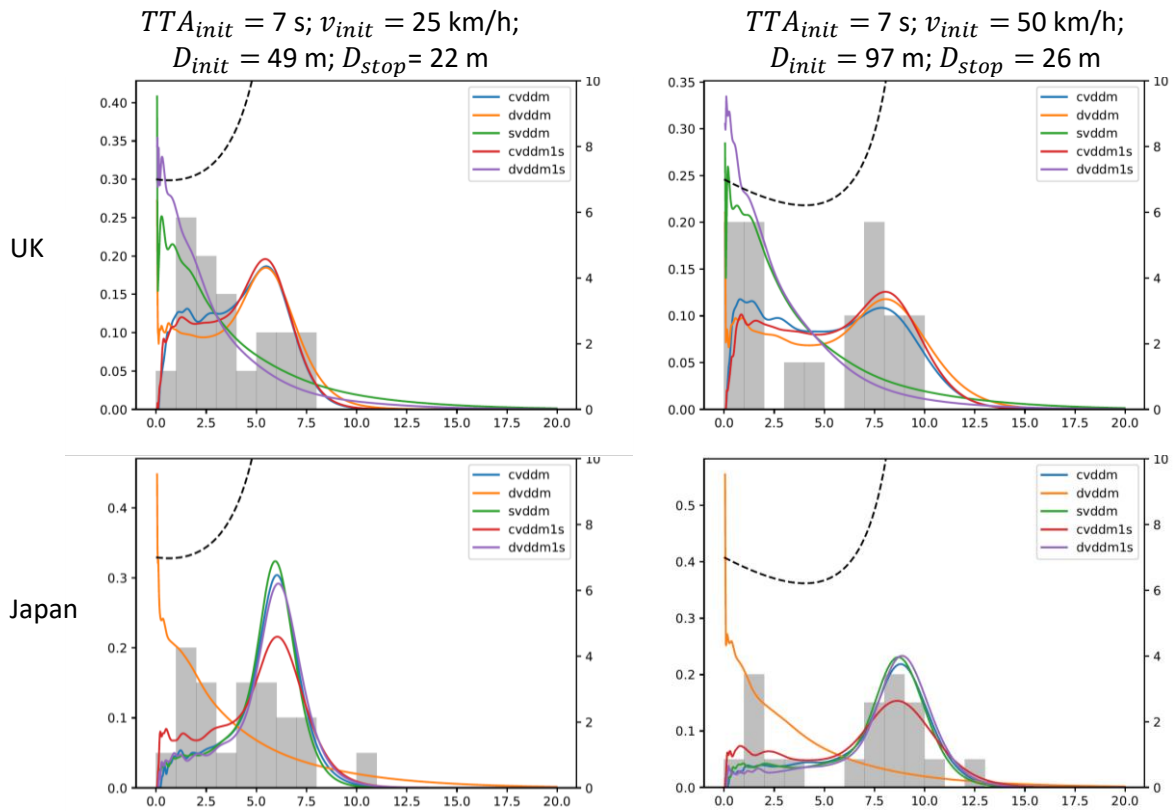


Figure 19: Human driver turning times (gray bars) and probability distribution predictions by fitted VDDM variants (solid lines), across time elapsed in the scenario (x axis, seconds), in two example *Decelerate to a stop* scenarios with same TTA_{init} but different v_{init}, D_{init} , and D_{stop} . The dashed lines show TTA during the scenario (right y axis, seconds).

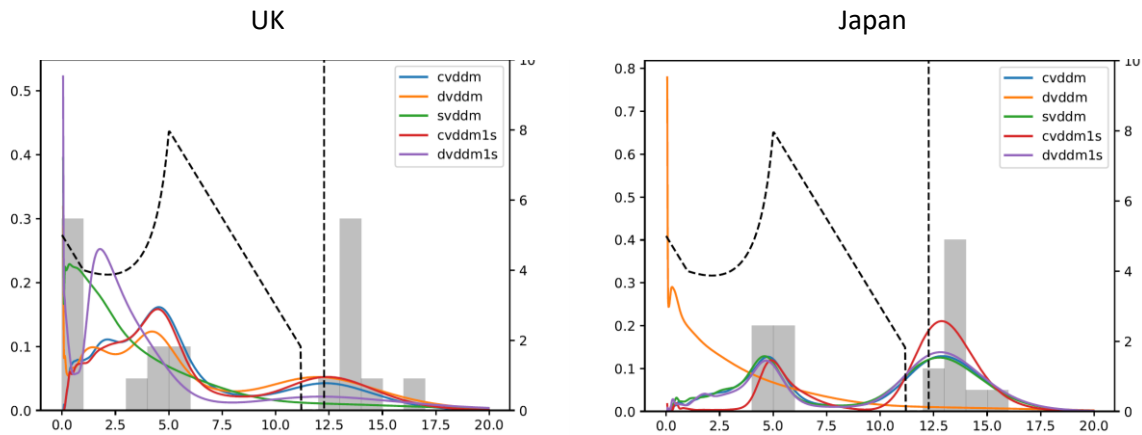


Figure 20: Human driver turning times (gray bars) and probability distribution predictions by fitted VDDM variants (lines), across time elapsed in the scenario (x axis, seconds), in the *Decelerate without stopping* scenario with $TTA_{init} = 5$ s. The dashed lines show TTA during the scenario (right y axis, seconds).

4.3.2 Statistical analyses of the impact of distance and deceleration cues on behaviour

To follow up on the above-mentioned indications of a distance-dependence in crossing decision timing, especially in the driver turning scenario, a further statistical analysis was carried out. This analysis made use of the pairs of *Constant velocity* scenario variants with identical TTA_{init} but distinct D_{init} , calculating for each such pair the fraction of participants crossing earlier in the scenario variant with higher D_{init} . If participants did not make use of distance cues to make their crossing decisions, we would expect this fraction to be statistically indistinguishable from 50%, but if they did make use of distance cues, we would expect fractions $>50\%$. Table 11 and Table 12 show the results for the pedestrian crossing and driver turning scenarios, along with p-values for a binomial test of the 50% fraction null-hypothesis in each case.

For the pedestrian crossing scenario, there is clear evidence of a distance-dependency for the two lower TTAs, up to $TTA_{init} = 4.58$ s (see Figure 15 for an illustration of this specific pair of scenarios). The observed fractions of early crossing in high D_{init} scenarios were larger in the UK dataset than in the Japanese dataset. This may be related to the overall tendency of the Japanese participants to cross later than the UK participants, such that a larger fraction of the Japanese participants crossed after the vehicle had already passed; for these participants we would not expect to see an effect of the initial vehicle distance. For the highest $TTA_{init} = 6.87$ s, there seemed to be a plateau effect where fractions of earlier crossing in the high D_{init} scenario dropped toward 50%. In line with previous literature (e.g., Lobjois and Cavallo, 2007), for these high distances and TTAs the crossing

decision seems to have been an easy one for the participants, resulting in very quick crossing decisions overall, such that effects of individual sensory cues become hard to disentangle.

For the driver turning scenario, the evidence of distance-dependency is clear across all initial TTAs tested, including $TTA_{init} = 6.5$ s, presumably because of the longer time needed to complete the crossing in this scenario, compared to the pedestrian crossing (see Figure 18 for an illustration of the $TTA_{init} = 6$ s scenario variants).

Table 11: Effect of the approaching vehicle’s initial distance on pedestrian crossing timing.

TTA_{init} (s)	Low D_{init} (m)	High D_{init} (m)	Fraction of participants crossing earlier in high D_{init} scenario					
			UK (n = 20)		Japan (n = 20)		Pooled (n = 40)	
			%	p	%	p	%	p
2.29	15.90	31.81	75.0%	0.0414	68.4%	0.1671	71.8%	0.0095
4.58	31.81	63.61	80.0%	0.0118	65.0%	0.2632	72.5%	0.0064
6.87	47.71	95.42	55.0%	0.8238	55.6%	0.8145	55.3%	0.6271

Table 12: Effect of the approaching vehicle’s initial distance on driver turning timing.

TTA_{init} (s)	Low D_{init} (m)	High D_{init} (m)	Fraction of participants crossing earlier in high D_{init} scenario					
			UK (n = 20)		Japan (n = 20)		Pooled (n = 40)	
			%	p	%	p	%	p
3.0	20.83	41.67	65.0%	0.2632	85.0%	0.0026	75.0%	0.0022
6.0	41.67	83.33	80.0%	0.0118	70.0%	0.1153	75.0%	0.0022
6.5	45.14	90.28	70.0%	0.1153	75.0%	0.0414	72.5%	0.0064

Another type of cue of interest, which the VDDMs as studied here did consider by means of the $\dot{\tau}$ input, relates to deceleration of the approaching vehicle. For the pedestrian crossing scenario (but not the driver turning scenario), there were two pairs of *Decelerate to a stop* scenario variants which differed internally only in terms of the final stopping distance D_{stop} , i.e., different magnitudes of deceleration were applied. Table 13 shows the results of a similar analysis to the ones reported above, showing that for the lower $TTA_{init} = 2.29$ s there is clear evidence of earlier pedestrian crossing with higher deceleration (higher D_{stop}). It should be noted however that this finding does not provide direct evidence for the use by participants of something like the $\dot{\tau}$ cue, since with higher decelerations also τ itself increases more quickly. Indeed, inspecting the results for the $TTA_{init} = 2.29$ s scenario variants in more detail, it is clear that a large proportion of the crossing decisions happened once the vehicle was almost or completely stopped, at which point τ is high, and this naturally happens earlier in the scenario variant with higher D_{stop} . For the scenario pair with higher $TTA_{init} = 4.58$ s (illustrated in Figure 16) there were no indications from the binomial tests that deceleration magnitudes affected the crossing decision timing. The TDM results in the next section further explore the impact of deceleration cues.

Table 13: Effect of the approaching vehicle’s final stopping distance on pedestrian crossing timing.

TTA_{init} (s)	Low D_{stop} (m)	High D_{stop} (m)	Fraction of participants crossing earlier in high D_{stop} scenario					
			UK (n = 20)		Japan (n = 20)		Pooled (n = 40)	
			%	p	%	p	%	p
2.29	4	8	80.0%	0.0118	90.0%	0.0004	85.0%	<0.0001
4.58	4	8	40.0%	0.5034	70.0%	0.1153	55.0%	0.6358

4.3.3 Model fits for the threshold distribution models

As mentioned, for the TDMs a full combinatorial set of model variants (16 different variants with different combinations of free/fixed parameters) was fitted to each of the four datasets (two scenarios, two countries). Examining the results from this detailed analysis, both in terms of log likelihoods, AICs, and produced probability distributions, the following four model variants were identified as an instructive subset to present in detail here:

- 5-parameter TDM: The simplest TDM, including just the lognormal distributions for $\tilde{\tau}_{pass}$ and T_R as well as the $\tilde{\tau}_{passed}$ threshold as free parameters. In other words, this model just responds to TTA, and initiates crossing once TTA exceeds a threshold from a distribution, further delayed by a reaction time distribution.
- 6-parameter TDM: Including also deceleration-dependency in the $\tilde{\tau}_{pass}$ quantity (adding k as a free parameter).
- 7-parameter TDM: Including also distance-dependency (adding p as a free parameter).
- 9-parameter TDM: Including also speed-dependency and the uniform slack distribution (adding q and P_{slack} as free parameters), i.e., the full model as described in Section 4.2.2.

In the tables below, as in Section 4.3.1, # denotes model parameter count, $\log(L)$ and AIC are goodness-of-fit indicators, with respectively larger (smaller negative) $\log(L)$ and smaller AIC values indicating more preferable models. The preferable model by AIC is indicated in bold face in each table. Fixed parameters are shown in grey font. The figures below showing model fits to example scenarios are for the same scenarios as in the corresponding figures for the VDDMs in Section 4.3.1.

Pedestrian crossing scenario

Table 14: TDM fits for the UK pedestrian crossing scenario. See the text for meanings of symbols and formatting.

Model	#	$\log(L)$	AIC	s_{pass}	m_{pass}	s_R	m_R	p	q	k	$\tilde{\tau}_{passed}$	P_{slack}
TDM 9	9	-438.6	895.3	0.774	34.489	0.561	0.964	2.291	2.248	17.334	-0.007	0.028
TDM 7	7	-452.4	918.7	0.586	27.802	0.662	1.010	1.470	1.000	13.121	-0.194	0.000
TDM 6	6	-453.9	919.7	0.422	4.604	0.647	1.040	1.000	1.000	1.625	-0.105	0.000
TDM 5	5	-484.0	978.1	0.479	3.495	0.769	0.916	1.000	1.000	0.000	-0.251	0.000

Table 15: TDM fits for the Japanese pedestrian crossing scenario. See the text for meanings of symbols and formatting.

Model	#	$\log(L)$	AIC	s_{pass}	m_{pass}	s_R	m_R	p	q	k	$\tilde{\tau}_{passed}$	P_{slack}
TDM 9	9	-533.9	1085.9	0.542	12.566	0.549	1.277	1.601	1.754	6.964	0.012	0.051
TDM 7	7	-542.8	1099.5	0.371	4.448	0.696	1.340	0.926	1.000	1.789	-0.055	0.000
TDM 6	6	-542.5	1097.1	0.377	6.146	0.683	1.391	1.000	1.000	2.881	0.049	0.000
TDM 5	5	-596.8	1203.6	0.559	4.244	1.002	1.028	1.000	1.000	0.000	-0.347	0.000

Overall, the fitting procedure for the TDMs seems to have worked better than the fitting procedure for the VDDMs, producing results that were mostly consistent between model variants and between separate fittings of individual variants. There were some indications of not always finding global likelihood maxima also for the TDMs, but these were mild in nature (note for example the slightly lower log likelihood for TDM 7 than TDM 6 in Table 15).

As can be seen in the figures further below, as with the VDDMs the TDMs generally managed well to capture the qualitative, multimodal nature of the pedestrian crossing time distributions. It was suggested above that the τ signal could seemingly explain this multimodality to a large extent, and the TDM 5 fits here, based on τ only, provide a direct illustration that this is indeed the case.

For the 5 and 6 parameter TDMs, the $\tilde{\tau}_{pass}$ distributions in Figure 21 are directly interpretable as distributions of TTA gaps accepted by the participants. The modes of the fitted $\tilde{\tau}_{pass}$ distributions with the 6-parameter model were 3.84 s and 5.25 s for UK and Japan, respectively. These values are generally in line with existing literature (e.g., Brewer et al, 2006; Lobois and Cavallo, 2007). A possible deviation from the literature is that the fitted $\tilde{\tau}_{pass}$ distributions taper off more slowly than what would be expected from other experiments. Lobois and Cavallo (2007) found that between-vehicle time gaps above 7-8 s were always accepted by their participants, Brewer et al. (2006), found 85th percentile gaps accepted to be about 6-8 s, whereas the TDMs fitted here assign a non-negligible probability to participants requiring gaps above 8 s, especially for the Japanese dataset. A likely reason for this finding is that the collected dataset did not include TTA_{init} values above 7 s. It should thus be noted that the fitted TDMs may produce more careful crossing behaviour than humans in scenarios with larger TTAs than what was studied empirically here.

The fitted reaction time (T_R) distributions were relatively consistent between model variants and datasets, generally having their mode around 0.4-0.7 s (mean 1.1-1.3 s), but with a tendency for longer T_R for the more complex models, especially the 9-parameter models.

For the VDDMs, we did not test a model variant without the \hat{v} deceleration cue, and the conventional statistical analyses above of the effect of deceleration cues were also inconclusive. The AIC analysis of the TDM variants, however, provided clear support for the inclusion of deceleration cues in the models, showing substantial reductions in AIC between the 5 and 6 parameter models. This improvement is clearly visible in the figures below showing scenarios with deceleration (Figure 23 and Figure 24) where the second crossing time mode of the 5-parameter model's distribution (blue line) occurs too late, since this model needs to wait for the τ signal to climb back above the initial TTA

before further crossings can be initiated (cf. Figure 14). The human participants often cross slightly earlier than this, at lower apparent TTAs, when there are signs of decelerations, and this behaviour is better captured by the 6-parameter model (orange line; sometimes hidden behind the green and red lines of the even more complex models). If anything, the humans seem to be using deceleration information to a greater extent than what the fitted models do.

The 7-parameter TDM, adding also the distance exponent parameter, does not seem recommendable over the 6-parameter model, since it increases the AIC for the Japanese dataset and only very slightly decreases it for the UK dataset.

In contrast, shifting to the full 9-parameter model does produce clear improvements in AIC, notably by setting both distance and speed exponents $p \approx q \approx 2$. The effect of such a parameterisation in practice is a subtle reshaping of the crossing time distributions, to have narrower peaks which fall back towards zero more quickly during times where few participants crossed. See for example around time 2.5 s in all four panels of Figure 23, where the 9-parameter model's distribution (red line) shows lower probabilities than all the other models. This type of model fit is an interesting finding, that could be worth further investigation and modelling. However, another implication of the exponentiation of τ in this model is that the entire $\tilde{\tau}_{pass}$ quantity becomes numerically inflated compared to the simpler models, with high values of especially m_{pass} and k . At present, we don't fully understand these aspects of the model, and there is a risk that the 9-parameter model is overfitting to the dataset at hand, and might "blow up" if generalised to new scenarios. For these reasons, and since the the 6-parameter and 9-parameter TDMs seem very similar in most aspects, for applied purposes we would recommend the simpler 6-parameter of the model for the time being.

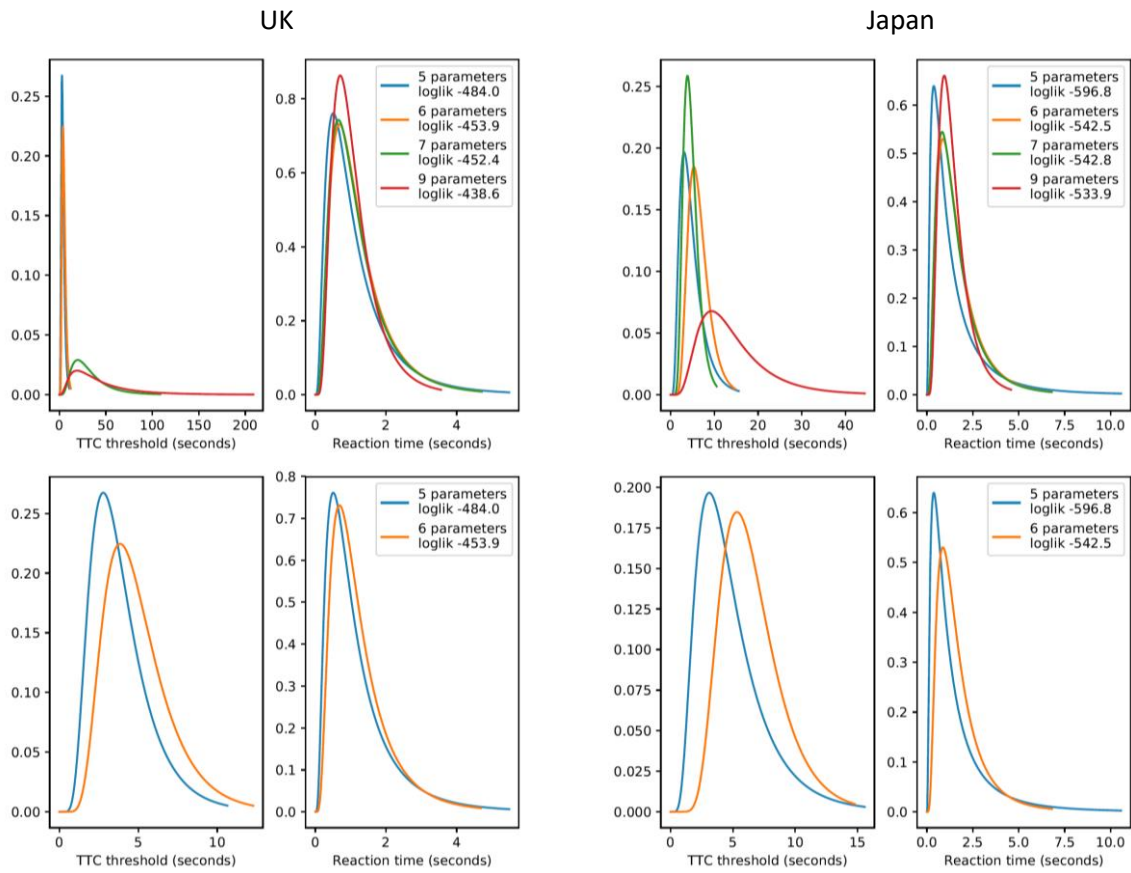


Figure 21: The $\tilde{\tau}_{pass}$ (generalised TTA or TTC) and T_R (reaction time) probability distributions obtained when fitting the TDMs to the UK (left two columns) and Japanese (right two columns) pedestrian crossing scenario.

The bottom row of panels shows the same as the top row, but only including the two simpler TDM variants. Note that for the models with more than 5 or 6 parameters, the $\tilde{\tau}_{pass}$ distribution is not clearly interpretable as time to arrival/collision. Also note that the different panels have different scale.

$$TTA_{init} = 4.6 \text{ s}; v_{init} = 25 \text{ km/h}; D_{init} = 32 \text{ m}$$

$$TTA_{init} = 4.6 \text{ s}; v_{init} = 50 \text{ km/h}; D_{init} = 64 \text{ m}$$

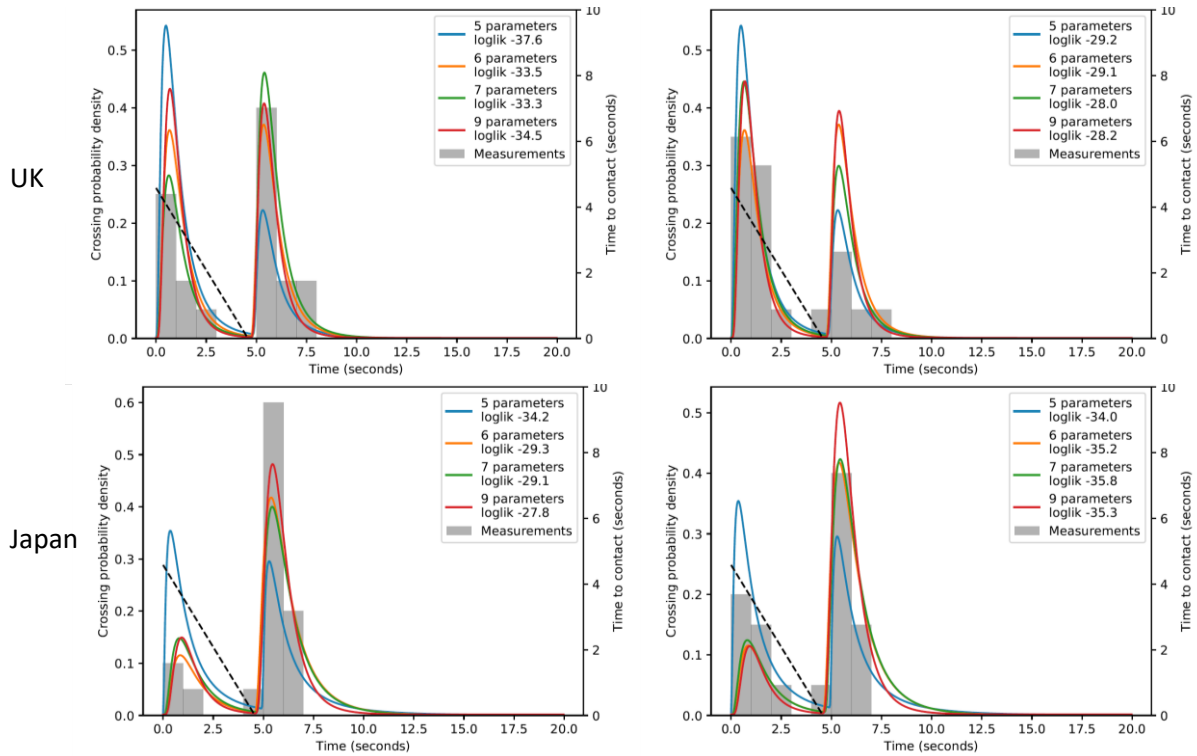


Figure 22: Human pedestrian crossing times (grey bars) and probability distribution predictions by fitted TDM variants (solid lines), across time elapsed in the scenario (x axis, seconds), in two example *Constant velocity* scenarios with same TTA_{init} but different v_{init} and D_{init} . The dashed lines show TTA during the scenario (right y axis, seconds).

$TTA_{init} = 4.6 \text{ s}; v_{init} = 50 \text{ km/h}; D_{stop} = 4 \text{ m}$

$TTA_{init} = 4.6 \text{ s}; v_{init} = 50 \text{ km/h}; D_{stop} = 8 \text{ m}$

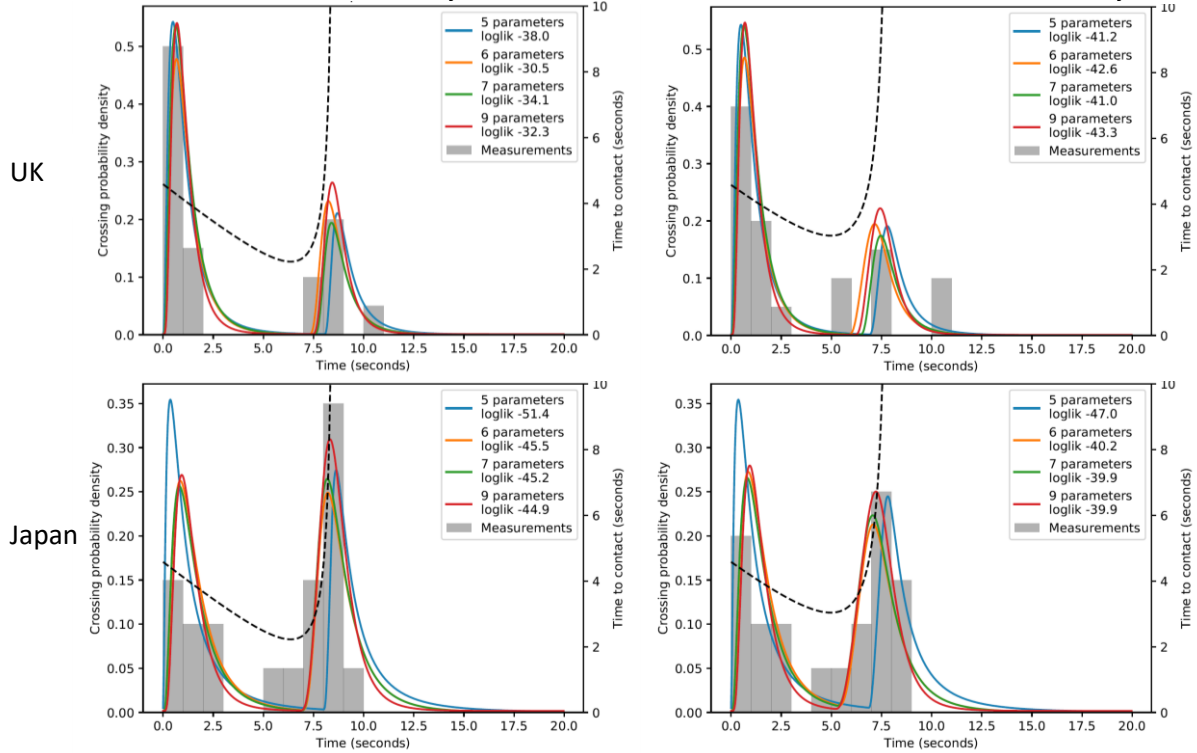


Figure 23: Human pedestrian crossing times (gray bars) and probability distribution predictions by fitted TDM variants (lines), across time elapsed in the scenario (x axis, seconds), in two example *Decelerate to a stop* scenarios with same TTA_{init} and v_{init} but different D_{stop} . The dashed lines show TTA during the scenario (right y axis, seconds).

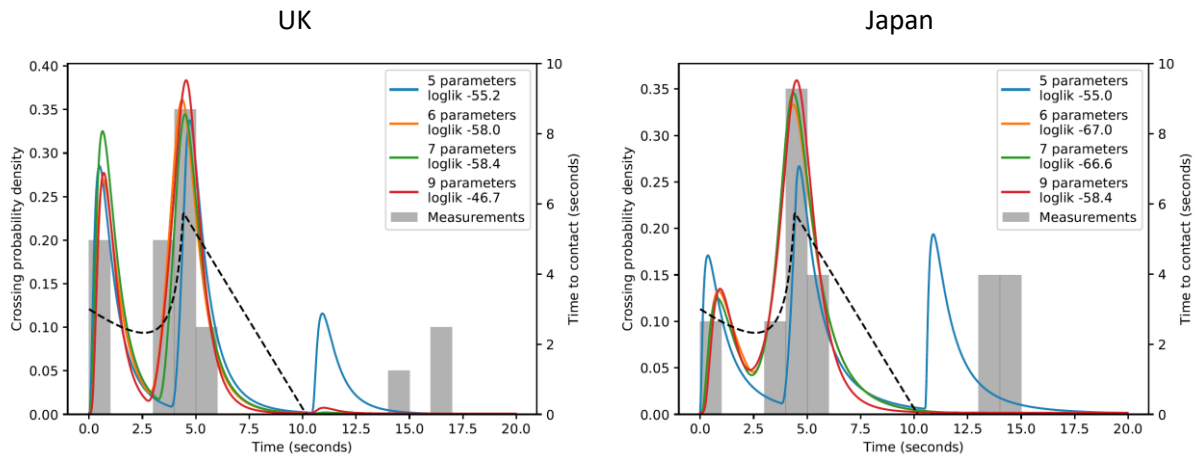


Figure 24: Human pedestrian crossing times (grey bars) and probability distribution predictions by fitted TDM variants (lines), across time elapsed in the scenario (x axis, seconds), in the *Decelerate without stopping* scenario with $TTA_{init} = 3$ s. The dashed lines show TTA during the scenario (right y axis, seconds).

Driver turning scenario

Table 16: TDM fits for the UK driver turning scenario. See the text for meanings of symbols and formatting.

Model	#	$\log(L)$	AIC	s_{pass}	m_{pass}	s_R	m_R	p	q	k	$\tilde{\tau}_{passed}$	P_{slack}
TDM 9	9	-486.4	990.7	0.495	7.487	0.524	1.114	1.012	1.067	0.604	0.954	9.2E-16
TDM 7	7	-486.5	986.9	0.494	6.827	0.535	1.095	0.951	1.000	0.552	0.934	0.000
TDM 6	6	-487.7	987.4	0.514	8.636	0.533	1.108	1.000	1.000	0.917	1.040	0.000
TDM 5	5	-508.3	1026.6	0.343	6.822	0.647	1.007	1.000	1.000	0.000	0.867	0.000

Table 17: TDM fits for the Japanese driver turning scenario. See the text for meanings of symbols and formatting.

Model	#	$\log(L)$	AIC	s_{pass}	m_{pass}	s_R	m_R	p	q	k	$\tilde{\tau}_{passed}$	P_{slack}
TDM 9	9	-442.5	903.0	0.351	3.182	0.547	1.043	0.650	0.848	0.046	0.471	2.7E-36
TDM 7	7	-442.7	899.3	0.422	4.113	0.530	1.075	0.776	1.000	0.100	0.436	0.000
TDM 6	6	-447.2	906.4	0.460	11.424	0.580	1.033	1.000	1.000	0.890	0.578	0.000
TDM 5	5	-469.9	949.9	0.301	8.202	0.725	0.913	1.000	1.000	0.000	0.468	0.000

Also in the driver turning scenario, the TDMs capture the multimodality of the human crossing time distributions rather nicely. The fits shown in the figures below are arguably still not quite as visually pleasing as for the pedestrian crossing scenario, but there is nevertheless a big improvement compared to the VDDMs. Comparing for example Figure 19 and Figure 27, it is clear that the TDMs managed to reproduce the bimodality of the human driver turning times in these scenarios, whereas the VDDMs did not.

As expected, the fitted $\tilde{\tau}_{pass}$ distributions predicted higher accepted time gaps than for the pedestrian crossing, again with higher values for the Japanese dataset than the UK dataset, with

modes at 9.29 s and 6.67 s, respectively, for the 6-parameter TDM. The UK value seems reasonably in line with previous literature, but the Japanese values seems large. In previous studies of US left turns across traffics, Mahmassani and Sheffi (1981) reported average size of accepted first gaps at around 7 s, and Chan et al. (2005) reported median accepted gap sizes at around 5 s. Just as for the pedestrian crossing scenario, there is a limitation in the scenarios studied empirically here, in that the largest initial TTA studied was 7 s, and again the obtained fits suggest that the models may generalise to over-cautious behaviour for scenarios with longer TTAs.

Again just as for the pedestrian crossing models, the obtained T_R distributions were relatively consistent between datasets and model variants. In fact, the obtained T_R distributions were rather similar to the ones obtained for the pedestrian crossing models, which is an interesting finding in its own right.

Furthermore, there were clear goodness-of-fit improvements from including deceleration cues in the models also for this scenario. These improvements are perhaps not as striking in the distribution figures below as they were for the pedestrian crossing data; the start of the second peak of crossing in deceleration scenarios does not move as much here. Instead, the improvement can be more clearly seen as a tendency of the 5-parameter model to cross before the approaching vehicle too often across most scenarios, presumably a trade-off to achieve reasonable fits on the scenarios with deceleration, also without model access to the deceleration cues.

Here, the 7-parameter model was the overall preferable model from an AIC perspective, across both datasets, although only marginally so over the 6-parameter model in the UK case. In the Japanese case there was a more notable overall difference in AIC, but per scenario variants the differences were very small, and the improvements did not come in the expected form. In Section 4.3.1 above, the pinpointed scenarios with a hoped-for improvement from distance cues were the ones shown here in Figure 26, with same TTA_{init} but different D_{init} . However, adding the distance exponent parameter did not reduce the early model crossing peak in the low D_{init} scenario; it actually slightly increased it instead. For these reasons, we are not sure that the addition of the distance exponent parameter did not lead to overfitting.

The 9-parameter model had worse performance, from an AIC perspective, than the 7-parameter model, and comparable performance to the 6-parameter model. The distance and speed exponents of this model were not fitted to above 1 as in the pedestrian crossing, which can be taken as possible support for the suspicion that those model fits for the pedestrian crossing scenario were overfits to the dataset at hand.

In sum, our recommendation here is again to use the 6-parameter model for applied purposes.

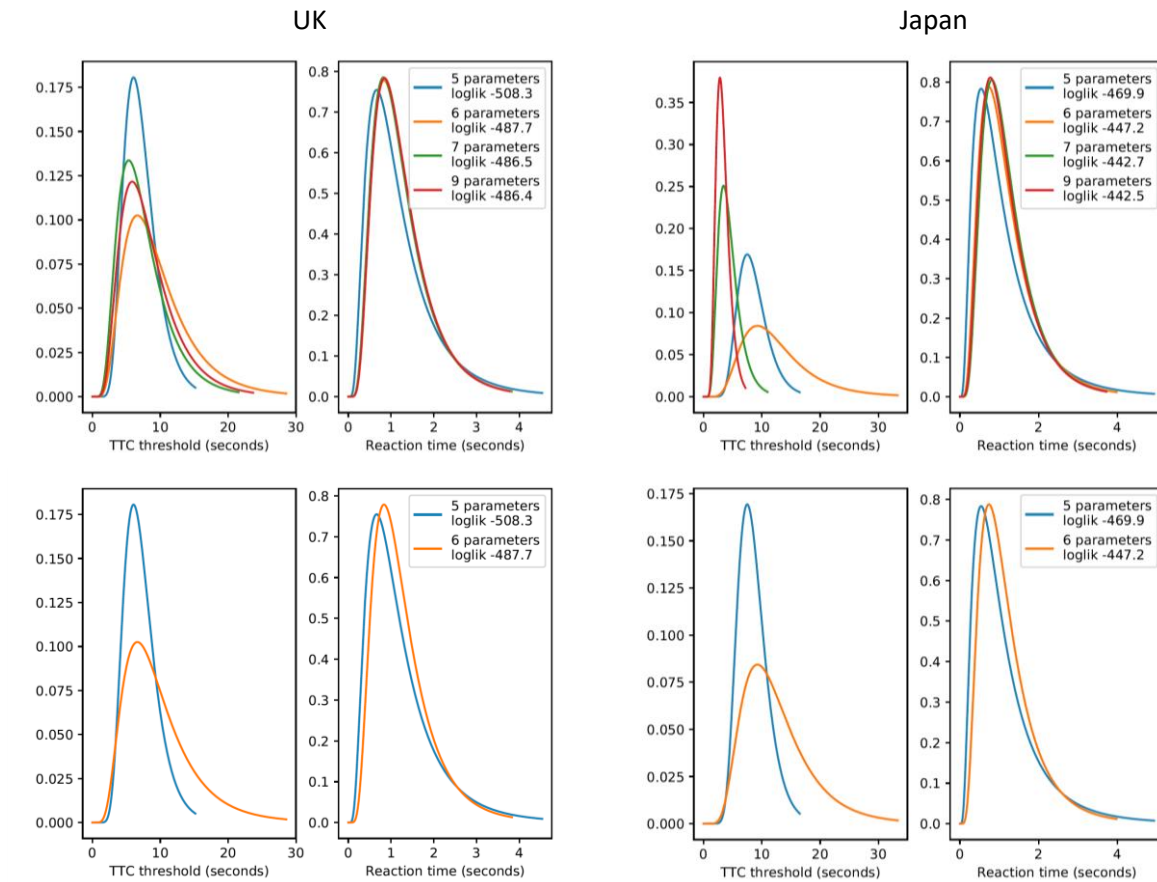


Figure 25: The $\tilde{\tau}_{pass}$ and T_R probability distributions obtained when fitting the TDMs to the UK (left two columns) and Japanese (right two columns) driver turning scenario. The bottom row of panels shows the same as the top row, but only including the two simpler TDM variants. Note that the different panels have different scale.

$TTA_{init} = 6\text{ s}; v_{init} = 25\text{ km/h}; D_{init} = 42\text{ m}$

$TTA_{init} = 6\text{ s}; v_{init} = 50\text{ km/h}; D_{init} = 83\text{ m}$

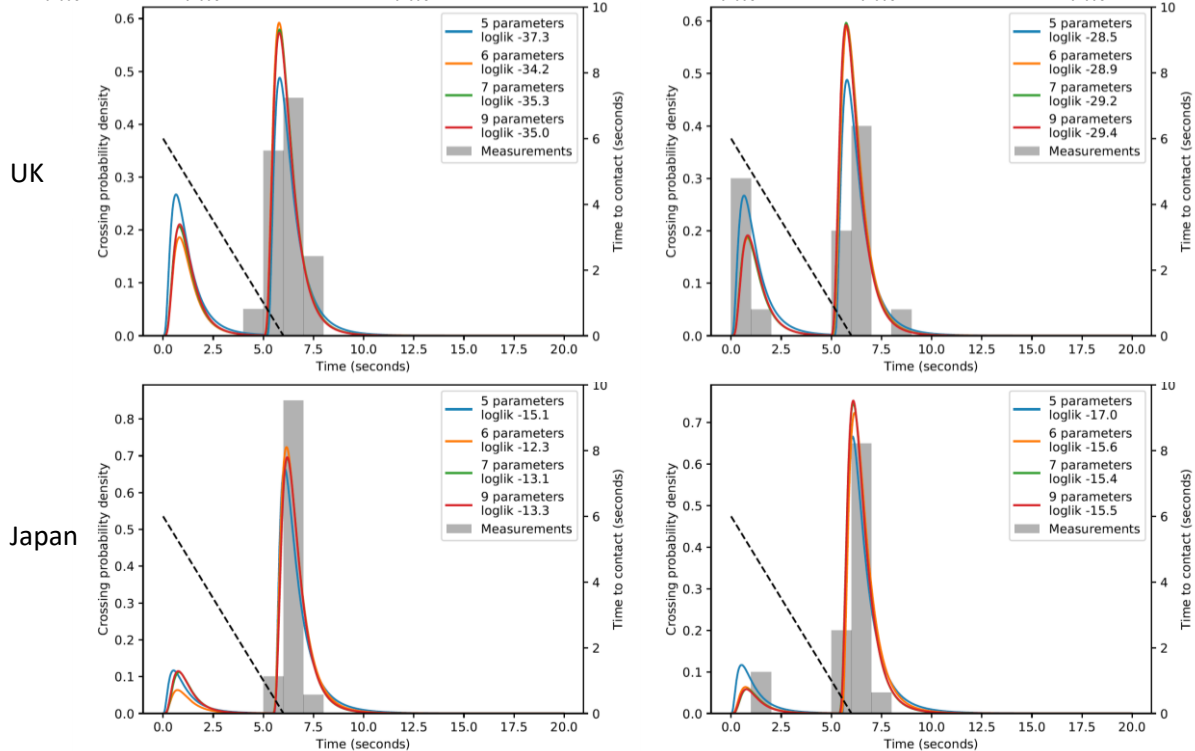


Figure 26: Human driver turning times (gray bars) and probability distribution predictions by fitted TDM variants (solid lines), across time elapsed in the scenario (x axis, seconds), in two example *Constant velocity* scenarios with same TTA_{init} but different v_{init} and D_{init} . The dashed lines show TTA during the scenario (right y axis, seconds).

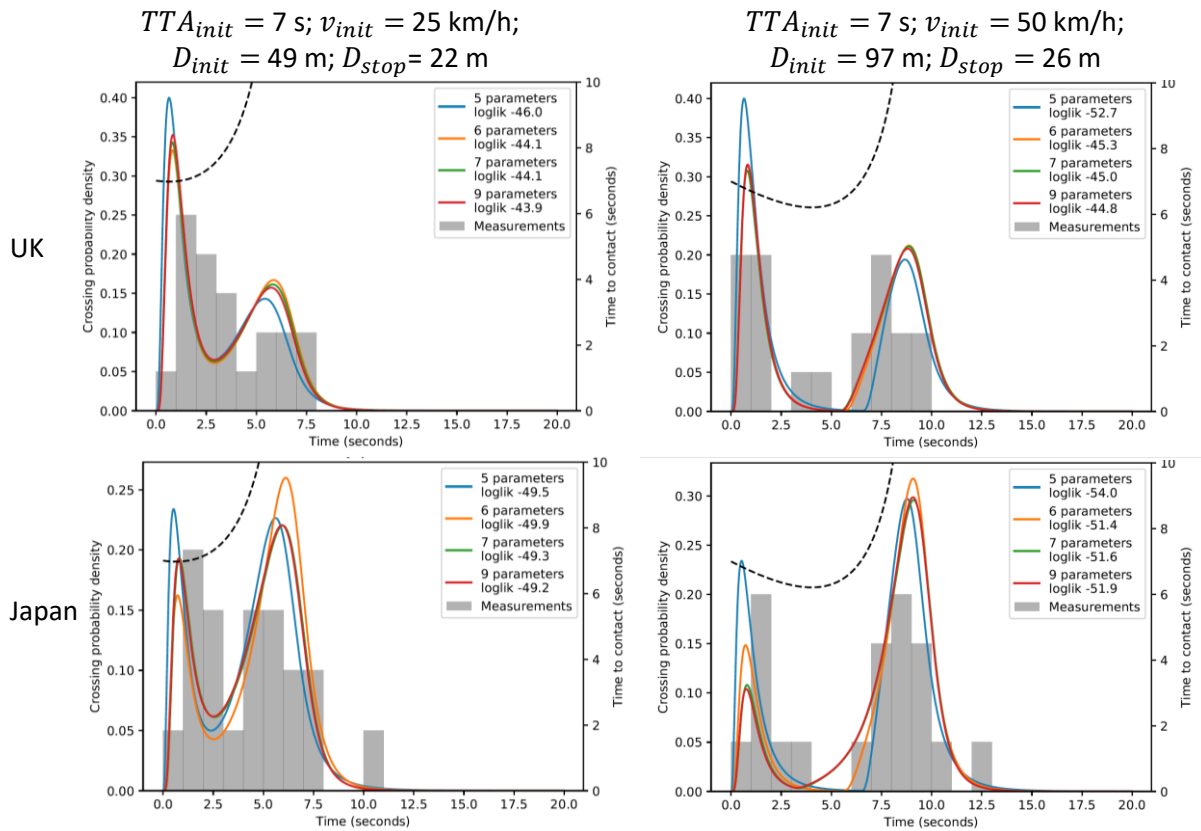


Figure 27: Human driver turning times (gray bars) and probability distribution predictions by fitted TDM variants (solid lines), across time elapsed in the scenario (x axis, seconds), in two example *Decelerate to a stop* scenarios with same TTA_{init} but different $v_{init}, D_{init},$ and D_{stop} . The dashed lines show TTA during the scenario (right y axis, seconds).

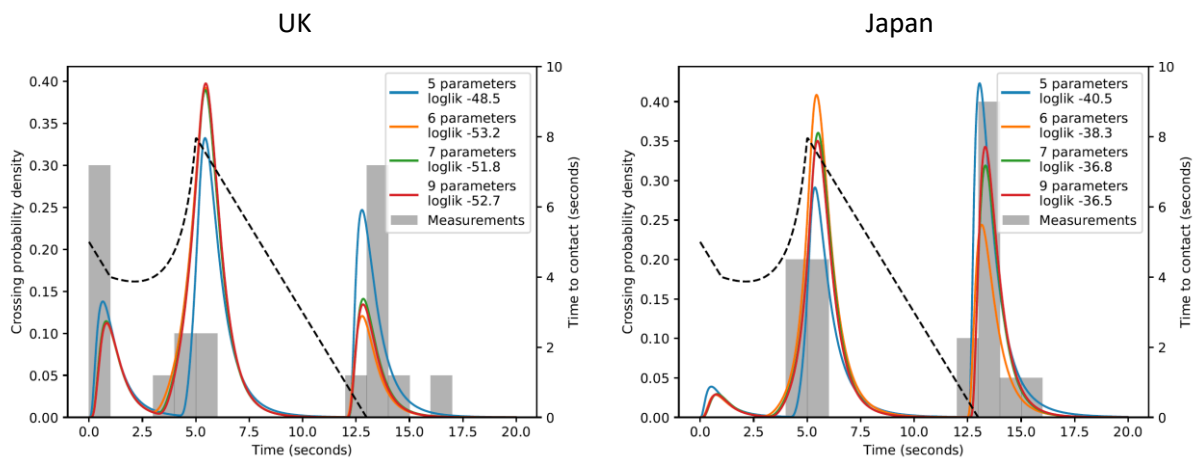


Figure 28: Human driver turning times (gray bars) and probability distribution predictions by fitted TDM variants (lines), across time elapsed in the scenario (x axis, seconds), in the *Decelerate without stopping* scenario with $TTA_{init} = 5$ s. The dashed lines show TTA during the scenario (right y axis, seconds).

4.3.4 Relationships between scenario kinematics and subjective safety ratings

Some preliminary analyses were also carried out into possible correlations between scenario kinematics and the subjective ratings of perceived safety provided by the participants after each road crossing. As mentioned in Section 4.2.1, the statement with which participants were asked to rate their agreement was “It was safe to cross before the vehicle”, on a Likert scale from “1: Strongly disagree” to “5: Strongly agree”.

Figure 29 and Figure 30 provide illustrations of these subjective ratings across three different example scenario variants for the pedestrian crossing and driver turning scenarios, respectively. These figures show pooled data across the UK and Japanese participants, since preliminary analyses suggested that there were no marked differences between the two.

One thing which stands out in these figures is that when participants crossed/turned after the approaching vehicle, they provided low ratings. Presumably, because of how the subjective safety statement was formulated, these low ratings reflect the participants’ decision, on these trials, to *not* pass before the vehicle.

More interesting, and of applied relevance, are the ratings from trials when participants did indeed pass before the approaching vehicle. For these trials, there are indications that participants reported lower perceived safety when initiating crossing/turning at lower apparent TTAs. See for example the top panel in Figure 29, UK where the earliest crossers, at apparent TTA over 4 s, provide safety ratings in the 3-5 range, whereas on crossings at apparent TTA between 2 and 4 s, the safety ratings were in the 1-4 range, with the value 3 seemingly most common. Also the driver turning data in Figure 30 align with this general pattern, but at higher TTAs overall, as expected; there are high safety ratings overall

for scenario in the middle panel, where TTAs were above 6 s throughout, and lower safety ratings in the other two scenarios, where TTAs were below 6 s.

There are also possible indications of deceleration cues playing into the safety ratings; note the high safety ratings at around 7 s and 3 s respectively in the scenarios in the middle and bottom panels of Figure 29, where apparent TTA is low, but where deceleration cues are strong.

Another interesting pattern is that participants often provided safety ratings lower than 5 also when passing in front of a completely stopped vehicle (middle panels in both figures below). One possible interpretation of this finding is that perceiving low TTAs during a vehicle approach elicits discomfort that persists for some time afterwards. Another possibility is that this finding is an artefact of the way the subjective safety statement was formulated here, potentially causing some participants to interpret the question as asking them whether it would have been safe to cross before the vehicle came to a full stop.

First attempts have been made at capturing the observed patterns in quantitative models mapping approach kinematics to subjective safety ratings. These models show some promise, but further work is needed, and ideally a better dataset where the subjective rating question is less open to differing interpretations between participants.

Constant velocity; $TTA_{init} = 4.6$ s; $v_{init} = 25$ km/h; $D_{init} = 32$ m

Decelerate to a stop; $TTA_{init} = 4.6$ s; $v_{init} = 50$ km/h; $D_{stop} = 4$ m

Decelerate without stopping; $TTA_{init} = 3$ s:

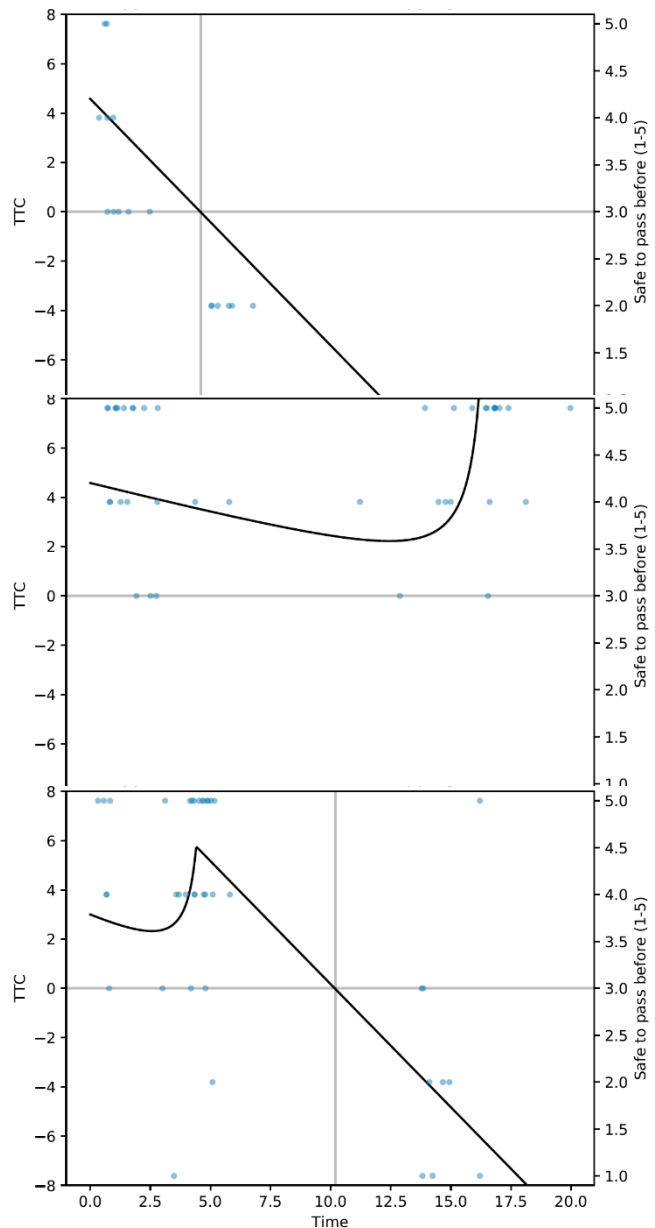


Figure 29: Subjective ratings of agreement with the statement “It was safe to cross before the vehicle” (blue dots) provided after trials from three different example pedestrian crossing scenarios, as a function of time at which the participants initiated crossing in the given trial. The solid line shows the apparent TTA of the vehicle during the scenario, i.e., $TTA = 0$ indicates that the approaching vehicle is just passing the participant.

Constant velocity; $TTA_{init} = 6$ s; $v_{init} = 50$ km/h; $D_{init} = 83$ m:

Decelerate to a stop; $TTA_{init} = 7$ s; $v_{init} = 50$ km/h; $D_{init} = 97$ m; $D_{stop} = 26$ m:

Decelerate without stopping; $TTA_{init} = 5$ s:

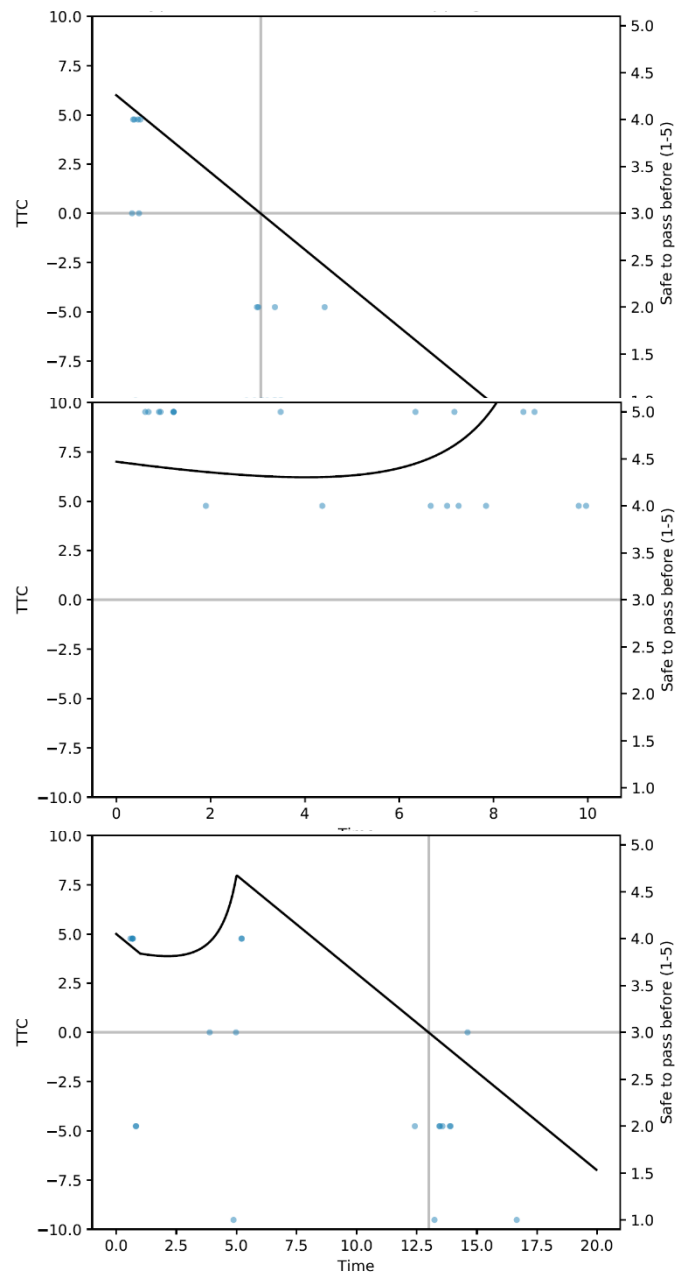


Figure 30: Subjective ratings of agreement with the statement “It was safe to cross before the vehicle” (blue dots) provided after trials from three different example driver turning scenarios, as a function of time at which the participants initiated turning in the given trial. The solid line shows the apparent TTA of the vehicle during the scenario, i.e., $TTA = 0$ indicates that the approaching vehicle is just passing the participant.

4.4 Conclusions

The sections below attempt to provide answers to each of the research questions defined in Section 4.1.

4.4.1 RQ1: Can the originally proposed VDDM framework capture the human behaviour in the studied crossing/turning scenarios?

For the pedestrian crossing scenario, the answer is yes; the VDDMs captured the human crossing behaviour both qualitatively and quantitatively. For the driver turning scenario the answer is less clear; the obtained VDDM fits were not satisfactory, but it is uncertain whether this was due to an inherent limitation of the model, or of the model fitting method used. The S-VDDM is similar in nature to the 6-parameter TDM (the latter can to some extent be seen as a computationally efficient approximation of the former). Therefore, it could be argued that the poorer performance of the S-VDDM than the 6-parameter TDM is likely to be a result of model fitting methods rather than the model formulation as such, but no firm conclusions can be drawn.

4.4.2 RQ2: Can the models be scaled down to less complex versions?

Yes, this was found to be the case. Firstly, in the sense that the less complex VDDM variants (e.g., S-VDDM) were comparable in performance to the more complex VDDM variants. Secondly, in the sense that the TDMs, which are arguably less complex than the VDDMs, also performed as well as the VDDMs.

4.4.3 RQ3: Can the same basic type of model be used both for pedestrian crossing and driver turning decision-making?

The TDMs were arguably not quite as successful for the driver turning scenario as they were for the pedestrian crossing scenario, but we would argue that they were successful enough to answer RQ3 with a tentative yes. Part of the reason why the TDMs were less successful for the driver turning scenario could be that the driver turning scenario variants in the experiment were not as appropriately defined as those for the pedestrian crossing scenario; not least coverage of longer TTAs would have been desirable in the driver turning experiments.

4.4.4 RQ4: Can the same basic type of model be used both for UK and Japanese road users, and if yes do the models need to be parameterised differently?

The answers to the both parts of this question are clearly positive. All model types were equally successful at reproducing the human behaviour as observed in both UK and Japan. Aligning with existing findings on Japanese pedestrians (Sueur et al., 2013), the Japanese participants were found

here to be consistently more careful in their decision-making, across both studied traffic scenarios, warranting the use of different model parameterisations for simulating UK and Japanese road users.

4.4.5 RQ5: To capture effects of available gap on crossing/turning behaviour, is it enough to consider only time to arrival, or should distance cues also be considered?

The statistical analyses here align with previous reports (Davis and Swenson, 2004; Lobjois and Cavallo, 2007; Yannis et al., 2013) of humans making use of not only time to arrival but also distance in determining whether a gap is large enough to permit crossing. Both in previous findings and in our experiments, larger distance gaps (or equivalently higher approach speeds) make humans more likely to accept a given time gap. This strongly suggests that models of crossing/turning decision-making should incorporate distance cues.

However, we have not been able here to find an appropriate formulation for how to incorporate distance cues into our models. Judging from the obtained fits, the models we provide are still useful in their current form, but extending them to incorporate distance cues would be desirable.

4.4.6 RQ6: To capture effects of vehicle deceleration on crossing/turning behaviour, is it enough to consider only time and/or distance gaps, or are direct cues describing deceleration also needed?

Yes, the model-fitting analyses of the TDMs strongly suggest that the human participants were able to pick up on deceleration of the approaching vehicle, and made use of this information in their crossing/turning decisions. The proposed 6-parameter TDM variants accounts for this phenomenon.

4.4.7 RQ7: Are there correlations between the kinematical conditions at crossing/turning and subjective ratings of perceived safety?

Our preliminary, qualitative analyses do suggest that this is the case, tentatively indicating (1) lower perceived safety when initiating crossing/turning at lower apparent TTAs, (2) effects of deceleration cues, and (3) possibly also persistence over time of discomfort from having perceived low TTAs. All three points, and especially the third one, warrant further investigation before any firm conclusions can be drawn.

4.5 Simulation software

The models described in this chapter have been packaged as MATLAB software, reusable by third parties. This software is provided as an addendum to this report, together with requisite documentation. The software includes a graphical user interface (GUI), shown in Figure 31, that can be used to easily define and run simulations, and visualise and study the results from various perspectives. Table 18 describes the types of analysis plots that can be accessed from within the GUI.

For more advanced uses, like for example searching for an optimum across a full range of possible AV approach behaviours, the software can also be used programmatically, without the GUI.

The models provided with the software are the 5-parameter and 6-parameter TDM variants; the GUI runs the 6-parameter version. The following known limitations of these models, discussed above in this chapter, should be borne in mind by users of the software:

- The models are likely to be over-cautious in their crossing/turning behaviour in scenarios with higher TTAs than 7 s (the highest TTA studied in our data collection experiments).
- The models do not consider distance cues. According to our findings, the models still account well for human crossing/turning behaviour across a wide variety of scenarios, but particularly the driver turning models seem more prone than humans to initiate turning at small distance gaps (low approach speeds) at TTAs where both humans and model would initiate turning at high TTAs; see Figure 26.

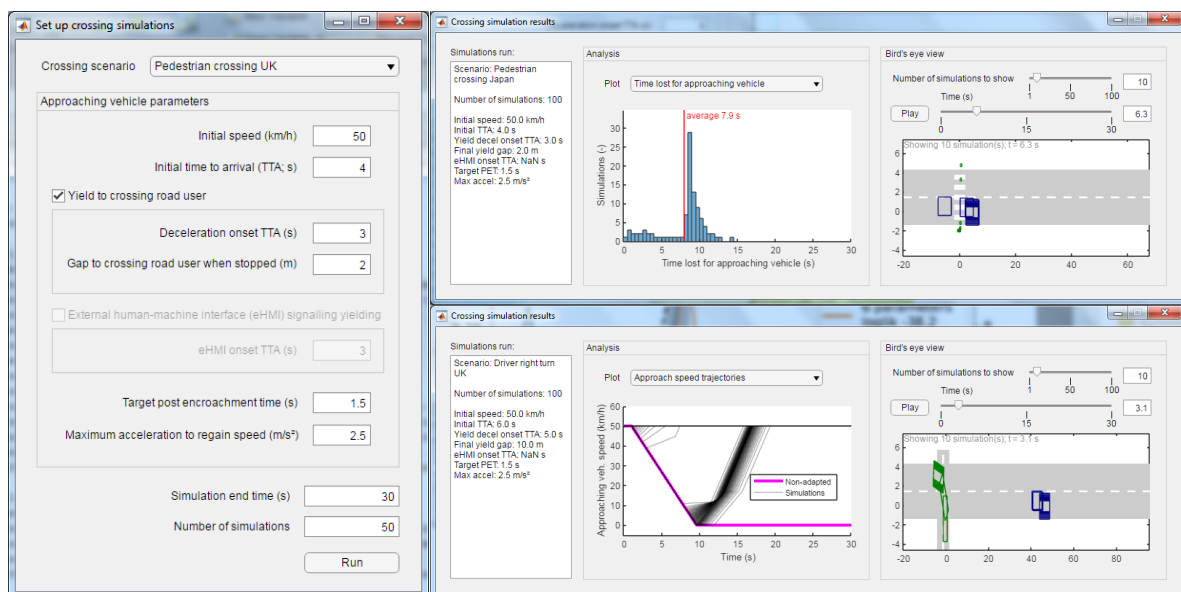


Figure 31: The graphical user interface of the road crossing behaviour simulation software provided with this deliverable.

Table 18: A listing of the types of analysis plots accessible via the simulation software GUI, together with explanations and possible interpretations and uses. A and C refer to the approaching and crossing/turning road users, respectively.

Plot	Explanation	Possible interpretation/use
Crossing onset times	Showing distributions (continuous and discrete) of simulation times at which the modelled road user C initiates crossing.	Larger values mean that C needed to wait longer before crossing.
Approach speed trajectories	Showing A's speed over time, both for the "non-adapted" case where A remains stationary after yielding to a full stop (or keeps initial speed in the non-yielding case), and for the actual model simulations where A also responds to C's crossing behaviour.	Reductions to lower speeds for A indicate a less efficient interaction.
Approach acceleration trajectories	As above, but for A's acceleration over time.	Large decelerations for A may have implications for comfort and safety for occupants in A, for C, and road users behind A.
Apparent TTA at crossing onset	Showing distributions of TTA for A, at the time at which C initiated crossing.	Smaller TTA values at crossing onset suggest an interaction that is potentially subjectively less safe for C (and any occupants in A).
Time lost for approaching vehicle	Showing distributions of the time delay for A as a result of the interaction (comparing A's distance travelled over time to a baseline case without road user C).	Larger delay times for A indicate a less efficient interaction.

4.6 Future work

There are many possible directions of work for further development of what has been presented here. One important next step, planned for interACT WP6, will be to apply the models developed here in impact analyses, to study the effects of different behaviours of AVs on traffic flow and objective and subjective safety (cf. Table 15). For these purposes, it will also be attempted to extend the models to factor in the impact of eHMI message on road user decisions. Another possible development that could be useful from this applied perspective, would be to extend the time frame in which the studied scenarios are modelled, to include for example also the turning/crossing road users' initial approach toward the interaction location.

Furthermore, it would be interesting in the future to attempt fitting the models also at the level of individual participants, rather than to an entire group of participants. This would however require experiments with more data points per participant. Finally, it would of course also be of interest to expand to address a larger set of traffic scenarios, but this is clearly beyond the scope of the interACT project.

5. Summary & outlook

This deliverable provides an insight into observing, understanding and modelling interaction in urban traffic. Generated data from the observational study was further analysed, showing that pedestrians base their crossing decision rather on implicit information from the vehicle than on explicit signals by the driver. Furthermore, explicit communication is more utilized in low speed scenarios such as shared spaces. Nonetheless, the adaptation of kinematic motion is a key indicator to indicate the intention to yield. A velocity threshold for interaction on main urban roads was identified: drivers are more willing to cooperate and thus yield their right of way if traffic is congested. In normal driving conditions, drivers on side roads or jaywalking pedestrians will use large enough gaps to reach their intended destination.

Simulator studies were conducted to research the individual effects of perceivable vehicle behaviour. Results indicate that the presence or attentiveness of a driver does not objectively influence the decision making, but influences perceived risk. The vehicle's pitch is a weak indication for a yielding intention compared to the onset of braking and the strategy involved. Defensive manoeuvres, i.e. stronger than needed decelerations in the beginning of a braking process, lead to quicker pedestrian crossing initiations. Therefore, the design of the vehicles trajectory when yielding right of way is an important factor to enable expectation conforming behaviour. eHMIs seem to expedite the decision making of other road users and could thus increase traffic flow. This will be further explored in the evaluation work of WP 6.

Quantitative models, described in D2.1, were reworked and fitted with data from multiple simulator experiments. A downscaling of the models showed a comparable performance to the more complex ones.

The identified effects of human-human and human-automation interaction will serve as an input the CCPU (WP 3,4,5) and for the evaluation studies planned within WP6 . Furthermore, data generated within the evaluation studies will be used to extend the quantitative models of interaction.

6. References

- Akaike, H. (1974). A new look at the statistical model identification. *IEEE Transactions on Automatic Control*, 19(6), 716-723.
- Brackstone, M., & McDonald, M. (1999). Car-following: a historical review. *Transportation Research Part F: Traffic Psychology and Behaviour*, 2(4), 181-196.
- Brewer, M. A., Fitzpatrick, K., Whitacre, J. A., & Lord, D. (2006). Exploration of pedestrian gap-acceptance behavior at selected locations. *Transportation Research Record*, 1982(1), 132-140.
- Chan, C. Y., Ragland, D. R., Shladover, S. E., Misener, J. A., & Marco, D. (2005). Observations of driver time gap acceptance at intersections in left-turn across-path–opposite-direction scenarios. *Transportation Research Record*, 1910(1), 10-19.
- Davis, G. A., & Swenson, T. (2004). Field study of gap acceptance by left-turning drivers. *Transportation Research Record*, 1899(1), 71-75.
- de Clercq, K., Dietrich, A., Núñez Velasco, J. P., de Winter, J., & Happee, R. (2019). External Human-Machine Interfaces on Automated Vehicles: Effects on Pedestrian Crossing Decisions. *Human Factors*. <https://doi.org/10.1177/0018720819836343>
- Crowley-Koch, B. J., Houten, R. and Lim, E. (2011). EFFECTS OF PEDESTRIAN PROMPTS ON MOTORIST YIELDING AT CROSSWALKS. *Journal of Applied Behavior Analysis*, 44: 121-126. doi:[10.1901/jaba.2011.44-121](https://doi.org/10.1901/jaba.2011.44-121)
- Dietrich, A., Bengler, K., Portouli, E. et al (2018). interACT Deliverable 2.1. Preliminary description of psychological models on human-human interaction in traffic. *EU H2020 project “Designing cooperative interaction of automated vehicles with other road users in mixed traffic environments”, grant number 723395*.
- Dietrich A., Maruhn P., Schwarze L., Bengler K. (2020) Implicit Communication of Automated Vehicles in Urban Scenarios: Effects of Pitch and Deceleration on Pedestrian Crossing Behavior. In: Ahram T., Karwowski W., Pickl S., Taiar R. (eds) Human Systems Engineering and Design II. IHSED 2019. *Advances in Intelligent Systems and Computing*, vol 1026. Springer, Cham
- Dietrich A., Ruenz J. (2019) Observing Traffic – Utilizing a Ground Based LiDAR and Observation Protocols at a T-Junction in Germany. In: Bagnara S., Tartaglia R., Albolino S., Alexander T., Fujita Y. (eds) Proceedings of the 20th Congress of the International Ergonomics Association (IEA 2018). *IEA 2018. Advances in Intelligent Systems and Computing*, vol 823. Springer, Cham
- Dietrich, A., Tondera, M., & Bengler, K., (submitted 2019). Automated vehicles in urban traffic: The effects of kinematics and eHMI on pedestrian crossing behaviour. *Road Safety and Simulation 2019*. Iowa City, USA.
- Dietrich, A., Willrodt, J.-H., Wagner, K. & Bengler, K. (2018). Projection-Based External Human Machine Interfaces – Enabling Interaction between Automated Vehicles and Pedestrians. *Proceedings of the DSC 2018 Europe VR, Driving Simulation & Virtual Reality Conference & Exhibition*, pp. 43-50, 2018.

- Gazis, D. C., Herman, R., & Rothery, R. W. (1961). Nonlinear follow-the-leader models of traffic flow. *Operations Research*, 9(4), 545-567.
- Giles, O., Markkula, G., Pekkanen, J., Yokota, N., Matsunaga, N., Merat, N., Daimon, T. (2019). At the Zebra Crossing: Modelling Complex Decision Processes with Variable-Drift Diffusion Models. *Proceedings of CogSci2019*, Montreal, Canada.
- Guéguen, N., Meineri, S., Eysartier, C. (2015). A pedestrian's stare and drivers' stopping behavior: A field experiment at the pedestrian crossing. *Safety Science*, Volume 75, 2015, Pages 87-89, ISSN 0925-7535. <https://doi.org/10.1016/j.ssci.2015.01.018>
- Himanen, V., Kulmala, R. (1988). An application of logit models in analysing the behaviour of pedestrians and car drivers on pedestrian crossings. *Accident Analysis & Prevention*, Volume 20, Issue 3, 1988, Pages 187-197, ISSN 0001-4575. [https://doi.org/10.1016/0001-4575\(88\)90003-6](https://doi.org/10.1016/0001-4575(88)90003-6)
- Jones, E., Oliphant, E., Peterson, P., et al. (2019). SciPy: Open Source Scientific Tools for Python, 2001-, <http://www.scipy.org/> [Online; accessed 2019-06-17]
- Lee, D. N. (1976). A theory of visual control of braking based on information about time-to-collision. *Perception*, 5(4), 437-459.
- Lee, Y.M., Madigan, R., Giles, O., Garach-Morcillo, L., Markkula, G., Fox, C., Camara F., Rothmueller, M., Vendelbo-Larsen, S.A., Rasmussen, P. H., Dietrich, A., Nathanael, D., Portouli, V., Schieben, A., & Merat, N. (under review). Road users rarely use explicit communication techniques when interacting in today's traffic: Implications for Automated Vehicles. *Cognition, Technology and Work*.
- Lee, Y.M., Uttley, J., Solernou, A., Giles, O., Markkula, G., Romano, R., & Merat, N. (2019). Investigating pedestrians' crossing behaviour during car deceleration using wireless head mounted display: an application towards the evaluation of eHMI of automated vehicles, New Mexico, *Driving Assessment*, 2019.
- Lee, Y.M., Uttley, J., Solernou, A., Giles, O., Markkula, G., Romano, R., & Merat, N. (in prep). Efficacy of virtual reality in pedestrians' crossing decision, behaviour and experience while judging different speeds, time gaps and deceleration of approaching vehicles.
- Lobjois, R., & Cavallo, V. (2007). Age-related differences in street-crossing decisions: The effects of vehicle speed and time constraints on gap selection in an estimation task. *Accident Analysis & Prevention*, 39(5), 934-943.
- Mahmassani, H., & Sheffi, Y. (1981). Using gap sequences to estimate gap acceptance functions. *Transportation Research Part B: Methodological*, 15(3), 143-148.
- Markkula, G., Romano, R., Madigan, R., Fox, C. W., Giles, O. T., & Merat, N. (2018). Models of Human Decision-Making as Tools for Estimating and Optimizing Impacts of Vehicle Automation. *Transportation Research Record*, 0361198118792131. <https://doi.org/10.1177/0361198118792131>
- Montufar, J., Arango, J., Porter, M., & Nakagawa, S. (2007). Pedestrians' normal walking speed and speed when crossing a street. *Transportation Research Record*, 2002, 90-97.

- Portouli E. et al. (2019) Methodologies to Understand the Road User Needs When Interacting with Automated Vehicles. In: Krömker H. (eds) *HCI in Mobility, Transport, and Automotive Systems. HCI 2019*. Lecture Notes in Computer Science, vol 11596. Springer, Cham
- Powell, M. J. D. (1964). An efficient method for finding the minimum of a function of several variables without calculating derivatives. *The Computer Journal* 7: 155-162.
- Riemersma, J. B. J. (1979). Perception in traffic. *Urban Ecology*, 4(2), 139-149.
- SAE International Surface Vehicle Recommended Practice, "Taxonomy and Definitions for Terms Related to Driving Automation Systems for On-Road Motor Vehicles", *SAE Standard J3016*, Rev. Jun. 2018.
- Sucha, M., Dostal, D., Risser, R. (2017). Pedestrian-driver communication and decision strategies at marked crossings. *Accident Analysis & Prevention*, Volume 102, 2017, Pages 41-50, ISSN 0001-4575. <https://doi.org/10.1016/j.aap.2017.02.018>
- Sueur, C., Class, B., Hamm, C., Meyer, X., & Pelé, M. (2013). Different risk thresholds in pedestrian road crossing behaviour: a comparison of French and Japanese approaches. *Accident Analysis & Prevention*, 58, 59-63.
- Várhelyi, A. (1998). Drivers' speed behaviour at a zebra crossing: a case study. *Accident Analysis & Prevention*, Volume 30, Issue 6, 1998, Pages 731-743, ISSN 0001-4575, [https://doi.org/10.1016/S0001-4575\(98\)00026-8](https://doi.org/10.1016/S0001-4575(98)00026-8)
- Velasco, J.P., Lee, Y.M., Uttley, J., Solernou, A., Farah, H., van Arem, B., Hagenzieker, M., & Merat, N., (2019). Interactions with automated vehicles: The effect of drivers' attentiveness and presence on pedestrians' road crossing behaviour, *Road Safety and Simulation* 2019.
- Wahde, M. (2008). Biologically inspired optimization methods: an introduction. *WIT Press*.
- Wales, D. J., and Doye, J. P. K. (1997). Global Optimization by Basin-Hopping and the Lowest Energy Structures of Lennard-Jones Clusters Containing up to 110 Atoms. *Journal of Physical Chemistry A*, 101, 5111.
- Watzlawick, P., Beavin, J. H., & Jackson, D. D. (2016). *Menschliche Kommunikation. Formen, Störungen, Paradoxien*, 13.
- Weber, F., Sorokin, L., Schmidt, E. et al. (2019). interACT Deliverable 4.2. Final interaction strategies for the interACT Automated Vehicles. *EU H2020 project "Designing cooperative interaction of automated vehicles with other road users in mixed traffic environments", grant number 723395*.
- Wilbrink, M., Schieben, A., Markowski, R. et al. (2018). interACT Deliverable 1.1. Definition of interACT use cases and scenarios. *EU H2020 project "Designing cooperative interaction of automated vehicles with other road users in mixed traffic environments", grant number 723395*.
- Yannis, G., Papadimitriou, E., & Theofilatos, A. (2013). Pedestrian gap acceptance for mid-block street crossing. *Transportation Planning and Technology*, 36(5), 450-462.

Annex 1: Road crossing behaviour models – simulation software

The full annex including the simulation software is available here:

<https://doi.org/10.17605/OSF.IO/49AWH>

Overview

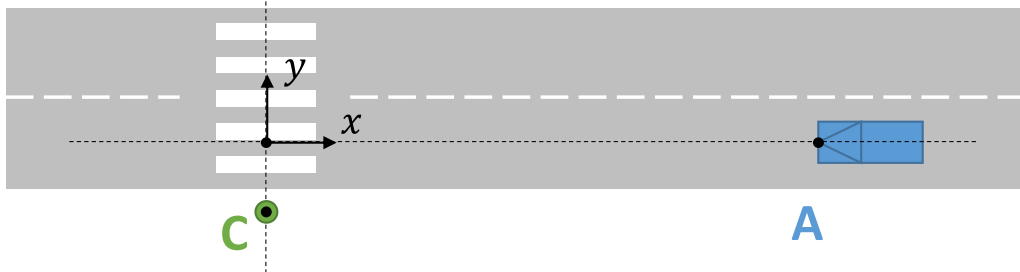
This addendum to interACT Deliverable D2.2 provides an implementation of the models developed in interACT WP2, and consists of the following:

- This document.
- A standalone Windows executable for running model simulations via a graphical user interface (GUI) – described in Section “Running model simulations from the GUI”² of this document.
- The MATLAB code underlying the standalone executable, allowing to build further on the software or to run more complex simulations (e.g., optimisations) programmatically – described in the last section of this document.

The interaction models developed in interACT WP2 address two scenario types, shown in Figure 32 below. As can be noted, both scenarios are of the nature that one crossing road user C intends to cross the path of an approaching vehicle A. In the context of interACT, the vehicle A may be an automated vehicle (AV), and the main intended use of the software provided here is to study how A’s behaviour affects the behaviour of C as well as the overall outcome of the interaction, for example from efficiency and safety perspectives. For a full description of the models and the empirical work supporting them, see interACT Deliverable D2.2.

In the rest of the report, *<base folder>* refers to the folder where you have unpacked the software.

Pedestrian crossing



Turning across traffic

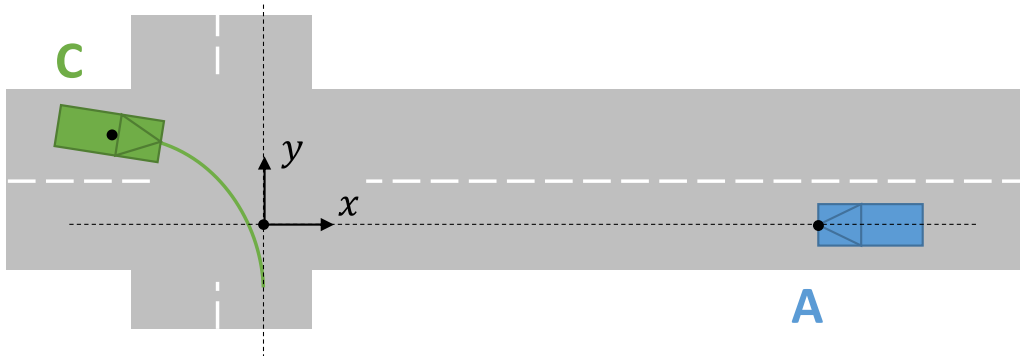


Figure 32: The two types of scenarios modelled in the simulation software.

Running model simulations from the GUI

There are a few different ways of starting the GUI:

1. If you have MATLAB R2017a or later installed on your computer, you can either
 - a. Run `<base folder>\executable\interACTRoadCrossingModels.exe`, or
 - b. Start MATLAB, make `<base folder>\source\` your current folder, and run `SetUpCrossingSimulations.mlapp`, either from the command prompt or by double clicking it from the “Current folder” file browser.
2. If you do not have MATLAB R2017a or later installed, run `<base folder>\installer\interACTRoadCrossingModels_installer.exe`. This installer will allow you to download the necessary MATLAB runtime files from the Internet and install the GUI executable where you want it on your computer.

Setting model parameters

Once the software runs, it will show the window in Figure 33.

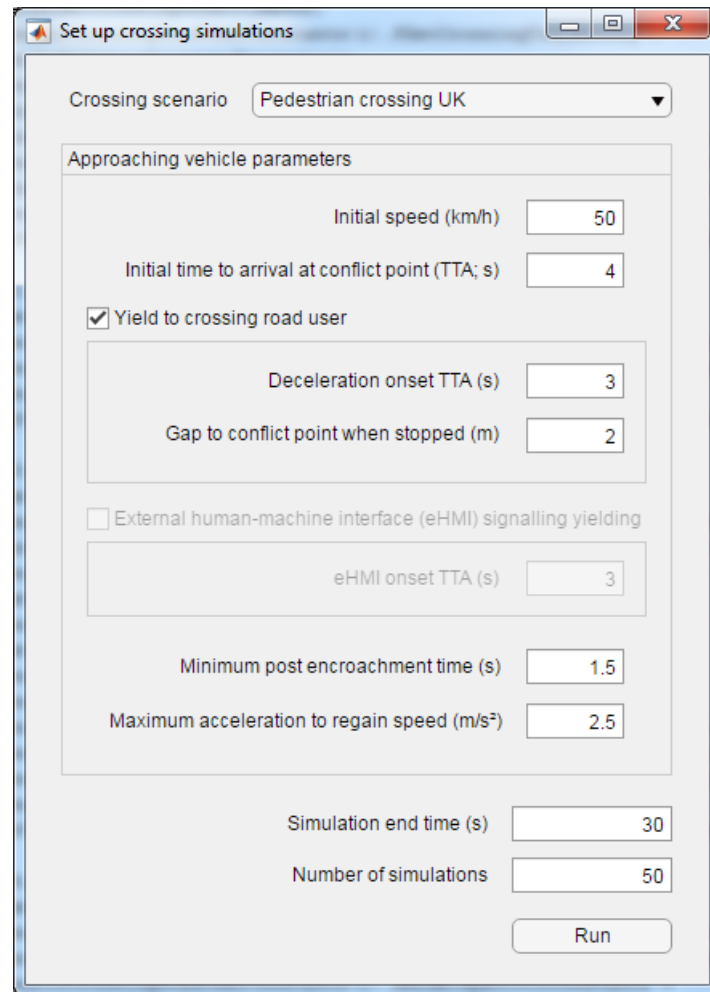


Figure 33: GUI for setting model parameters and running simulations.

The drop down menu at the top of this window allows you to choose between the two scenario types, and also between model parameterisations of the crossing road user C for the United Kingdom (UK) and Japan. The models run by the GUI are the 6-parameter threshold distribution models (TDMs) described in Deliverable D2.2.

The panel “Approaching vehicle parameters” allows you to define the behaviour of the approaching vehicle A. In the model simulations as provided here, the behaviour of A is as follows:

- The vehicle A has an *initial speed* at the start of a simulation, at an initial distance x from the crossing location (see Figure 32 for coordinate system), determined by the *initial time to arrival* ($TTA = \text{distance} / \text{speed}$) at the *conflict point*, which for both scenarios is the origin location of the coordinate system as shown in Figure 32. (Please note that this is a slightly different convention from how the scenario parameters were described in deliverable D2.2, where TTA was defined with respect to C’s position. For the pedestrian crossing this does not

make a difference, since the pedestrian moves along the y axis, but it does make a difference for the driver turning scenario, so to reproduce the results in D2.2 the TTAs need to be adjusted accordingly.)

- The vehicle A either does not yield to road user C, in which case the initial speed is maintained, or
- The vehicle A yields to C, by beginning to decelerate at a *deceleration onset TTA* (again relative to the conflict point), with a constant deceleration so as to reach zero speed at a certain *gap to the conflict point when stopped*.
- Regardless of A's prior behaviour, if at any point road user C begins crossing in front of A, A applies a constant deceleration so as to pass behind C at a *minimum post encroachment time* (PET = time between when C exits the area of overlap between A's and C's paths, and when A enters this area). Please note that the supplied model for A does not apply an upper limit to the magnitude of deceleration applied at this stage, so if C initiates crossing when A is near the conflict point, A may apply unrealistically large decelerations.
- If, after the above, A is at a lower speed than the initial speed, A applies a *maximum acceleration to regain speed*, until the initial speed is regained.

The final two fields in the window determine the duration of model simulations, and how many discrete simulations to run. The crossing behaviour model for C is essentially continuous in nature, but is sampled at a number of discrete locations, and A's response is then simulated at each of these.

Note that the GUI elements relating to eHMI are placeholders only; response to eHMI messages is not supported by the current version of the models.

Each time you press the "Run" button a new window such as in Figure 34 below will open, showing model simulation results for the model parameters you selected. You can do this repeatedly without closing the results windows, modifying model parameters between each time, to compare the interaction outcome between windows and thus see the impact of the parameter modifications.

Exploring simulation results

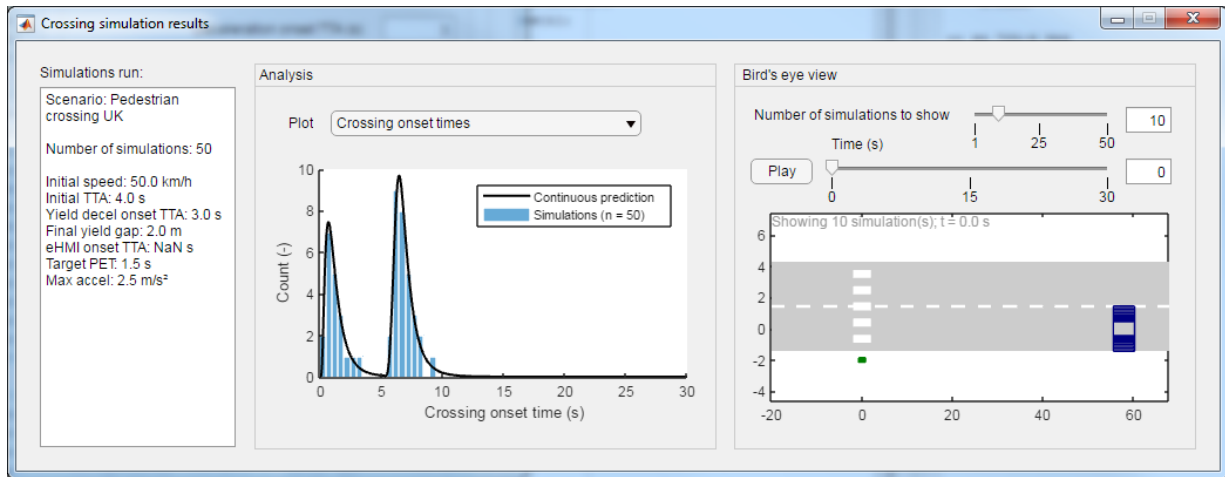


Figure 34: GUI for exploring model simulation results.

The simulation results window has three main parts:

Firstly, a text box to the left, summarising the model parameters used for the simulations.

Secondly, an “Analysis” panel in the middle, providing a drop down menu choosing between different plots:

Plot	Explanation	Possible interpretation/use
Crossing onset times	Showing distributions (continuous and discrete) of simulation times at which the modelled road user C initiates crossing.	Larger values mean that C needed to wait longer before crossing.
Approach speed trajectories	Showing A’s speed over time, both for the “non-adapted” case where A remains stationary after yielding to a full stop (or keeps initial speed in the non-yielding case), and for the actual model simulations where A also responds to C’s crossing behaviour.	Reductions to lower speeds for A indicate a less efficient interaction.
Approach acceleration trajectories	As above, but for A’s acceleration over time.	Large decelerations for A may have implications for comfort and safety for occupants in A, for C, and road users behind A.
Apparent TTA at crossing onset	Showing distributions of TTA for A, at the time at which C initiated crossing.	Smaller TTA values at crossing onset suggest an interaction that is potentially subjectively less safe for C (and any occupants in A).

Time lost for approaching vehicle	Showing distributions of the time delay for A as a result of the interaction (comparing A's distance travelled over time to a baseline case without road user C).	Larger delay times for A indicate a less efficient interaction.
-----------------------------------	---	---

Thirdly, a “Bird’s eye view” panel to the right, providing a direct visualisation of the simulations. All or a subset of the discrete simulations can be visualised at the same time. For increased clarity, when more than one simulation is shown, road users are shown as “spread out” laterally by small distances relative to their true locations in the simulations. There is also the possibility to play/pause the scenario as an animation. In the current version of the software, it is not possible to play animations in several results windows simultaneously.

Running model simulations programmatically

Before running model simulations programmatically, it is probably a good idea to read Section 2 above and to try out the GUI, to get acquainted with the models, simulations, and the types of analyses supported by the provided MATLAB code.

The code itself is available in `<base folder>\source\`. The main function to use to run simulations programmatically is the one defined in *SimulateCrossingScenario.m*:

```
function SSimulationResults = SimulateCrossingScenario(...
    SSimulationConstants, SApproachingRoadUserConstants, ...
    SCrossingRoadUserConstants)
```

The *SSimulationConstants* input structure defines the basic simulation settings (time step, duration, how many simulations to run). The other two input structures define pointers to user-provided functions implementing the model behaviour of approaching and crossing road users, as well as the parameters needed by those models. The *SSimulationResults* output structure contains fields both providing the original input structures, as well as various fields describing the simulation results, not least *SSimulationResults.SSimulations*, a structure array with one element per simulation, with fields providing vectors describing the movement of the two involved road users over time. All input and output variables use SI units. See *SimulateCrossingScenario.m* (or type [help SimulateCrossingScenario](#) at the MATLAB prompt) for further details about the input and output structures to *SimulateCrossingScenario*.

The main processing steps of the *SimulateCrossingScenario* function are:

1. Call the user-provided function *SApproachingRoadUserConstants.fGetApproachBehaviour* to get the baseline approach behaviour of A, without any adaptation to C.
2. Call the user-provided function *SCrossingRoadUserConstants.fGetCrossingOnsetTimePDF* to get the distribution of crossing onset times for C as a function of A’s approach behaviour.
3. For *i* over each of the *N* discrete simulations to run:

- a. Get the (i/N) th percentile (not exactly, see the code for the exact expression) of the crossing onset time distribution.
- b. Call the user-provided function *SCrossingRoadUserConstants.fGetCrossingTrajectory* to get a crossing trajectory for C starting at the crossing onset time obtained in the previous step.
- c. Call the user-provided function *SApproachingRoadUserConstants.fAdaptToCrossingBehaviour* to get a trajectory for A that is adapted to C's crossing trajectory.

The GUI provided with this software calls *SimulateCrossingScenario* with user-provided functions and associated model parameters defined so as to generate model behaviour described in Section 0 above. See *GetScenarioConstants.m* and *GetBaseApproachingRoadUserConstants.m* for a full view of how the models and scenarios implemented in the software as provided here were defined in the structures passed as input to the *SSimulationResults* function.

When using the *SimulateCrossingScenario* programmatically, the user can of course modify the user-provided functions according to own purposes, or provide entirely new functions.

The script in *test_SimulateCrossingScenario.m* illustrates how the *SimulateCrossingScenario* function can be used programmatically, recreating two of the scenario variants described in Deliverable D2.2. The script visualises the simulation results both by starting instances of the results visualisation GUI described in the previous section, as well as by creating MATLAB figures directly using some of the same analysis and plotting functions as the GUI, but without going via the GUI. The script also shows how to make the adjustments for the above-mentioned differences in reference frame between the simulation code and the driver turning scenario definitions in Deliverable D2.2.

For further details, see code comments in the various MATLAB files in `<base folder>\source\`.

For more information:

interACT Project Coordinator

Anna Schieben

DEUTSCHES ZENTRUM FUER LUFT - UND RAUMFAHRT e.V. (DLR)

Lilienthalplatz 7

38108 Braunschweig, Germany

Anna.Schieben@dlr.de

interact-roadautomation.eu/



Designing cooperative interaction of automated vehicles with
other road users in mixed traffic environments